IL-4 directly signals tissue-resident macrophages to proliferate beyond homeostatic levels controlled by CSF-1

IL-4 directly signals tissue resident macrophages to proliferate beyond homeostatic levels controlled by CSF-1.

Stephen J. Jenkins[1,2]*, Dominik Ruckerl[1], Graham D. Thomas[1§], James P. Hewitson[1], Sheelagh Duncan[1], Frank Brombacher[3], Rick M. Maizels[1], David A. Hume[4], and Judith E. Allen[1].

[1] University of Edinburgh
Institute of Immunology and Infection Research
School of Biological Sciences
Edinburgh
EH9 3JT
UK

[2] University of Edinburgh
Centre for Inflammation Research
College of Medicine and Veterinary Medicine
Edinburgh
EH16 4TJ
UK

[3] International Centre for Genetic Engineering and Biotechnology & University of Cape Town
IIDMM
Observatory 7925
Cape Town
South Africa

[4] University of Edinburgh
The Roslin Institute and Royal (Dick) School of Veterinary Studies
College of Medicine and Veterinary Medicine
Edinburgh
Midlothian
EH25 9RG
UK

[§]Current address:
La Jolla Institute for Allergy and Immunology
9420 Athena Cir La Jolla
CA 92037
USA

*Address for correspondence:
stephen.jenkins@ed.ac.uk
Tel: +44 (0)131 2426655
Fax: +44 (0)131 2426657

Running title: IL-4 drives macrophage proliferation

Summary caption: Independent IL-4 and CSF-1 mechanisms contribute to macrophage proliferation during nematode infection, but IL-4 permits increased tissue macrophage density without the co-incident monocyte infiltration associated with elevated CSF-1 levels.

Character Count: 39596

Non-standard abbreviations: GI, gastro-intestinal; IL-4c, IL-4 complex; IL-13c, IL-13 complex; *Hp*, *Heligmosomoides polygyrus*; *Ls*, *Litomosoides sigmodontis;* MΦ, macrophage.

Abstract

Macrophages (MΦ) colonize tissues during inflammation in two distinct ways; recruitment of monocyte-precursors and proliferation of resident cells. We recently revealed a major role for IL-4 in the proliferative expansion of resident MΦ during a Th2-biased tissue nematode infection. We now show that proliferation of MΦ during intestinal as well as tissue nematode infection is restricted to sites of IL-4 production and requires MΦ-intrinsic IL-4R signaling. However, both IL-4Rα-dependent and independent mechanisms contributed to MΦ proliferation during nematode infections. IL-4R-independent proliferation was controlled by a rise in local CSF-1 levels but IL-4Rα expression conferred a competitive advantage with higher and more sustained proliferation and increased accumulation of IL-4Rα^{+} compared to IL-4Rα^{-} cells. Mechanistically, this occurred by conversion of IL-4Rα^{+} MΦ from a CSF-1-dependent to CSF-1-independent program of proliferation. Thus, IL-4 increases the relative density of tissue MΦ by overcoming the constraints mediated by the availability of CSF-1. Finally, while both elevated CSF1R or IL-4Rα signaling triggered proliferation above homeostatic levels, only CSF-1 led to the recruitment of monocytes and neutrophils. Thus, the IL-4 pathway of proliferation may have developed as an alternative to CSF-1 in order to increase resident MΦ numbers without co-incident monocyte recruitment.

Introduction

The number of resident macrophages (MΦ) in several tissues can apparently be maintained without replenishment from blood monocytes and other hematopoietic precursors (Ajami et al., 2007; Kanitakis et al., 2004; Klein et al., 2007; Murphy et al., 2008; Schulz et al., 2012; Volkman et al., 1983; Yona et al., 2013) through in situ proliferation (Chorro et al., 2009; Davies et al., 2011; Hashimoto et al., 2013; Jenkins et al., 2011). Local proliferation restores homeostatic numbers of resident lung and peritoneal MΦ following their loss due to acute inflammation (Davies et al., 2011; Hashimoto et al., 2013) but can act also as an 'inflammatory' mechanism, leading to an outgrowth of tissue resident MΦ beyond homeostatic levels. For example, infection with the rodent filarial nematode *Litomosoides sigmodontis* (*Ls*) causes a pleuritis characterized by expansion of the resident MΦ population to high densities equivalent to that reached by recruited monocyte-derived MΦ during classical inflammation (Jenkins et al., 2011). Similarly, Langerhans cells and microglia increase in density via elevated self-renewal during atopic dermatitis and experimental autoimmune encephalitis, respectively (Ajami et al., 2011; Chorro et al., 2009).

Proliferation, differentiation and survival of MΦ is controlled by the CSF1R ligands CSF-1 and IL-34 produced by local tissue stroma to regulate the density of resident MΦ (Hume and MacDonald, 2011). CSF-1 administration to mice can increase blood monocyte and tissue MΦ numbers (Hume et al, 1988). Mice lacking the CSF1R exhibit an extreme deficit in resident MΦ in many tissues (Dai et al., 2002) and the same cells are ablated in a time-dependent manner following treatment with a blocking anti-CSF1R antibody (MacDonald et al., 2010). A proliferative signal through the CSF1R has been shown to maintain homeostatic numbers of resident peritoneal MΦ in the steady-state (Davies et al., 2013), and mediate repopulation of resident lung and peritoneal MΦ following acute inflammation or experimental depletion (Davies et al., 2013; Hashimoto et al., 2013). CSF1R signaling can also control in vivo proliferation of monocyte-derived MΦ, required for the population of the growing myometrium in pregnancy (Tagliani et al., 2011) or maintenance of recruited cells during the resolution phase of sterile peritonitis (Davies et al., 2013).

The Th2 lymphokine IL-4, was first shown to regulate proliferation and accumulation of resident MΦ in the context of filarial nematode infection. Moreover, serial administration of a rIL-4 complex (IL-4c) was sufficient to induce proliferation and accumulation of MΦ throughout the body, including in the peritoneal cavity and liver (Jenkins et al., 2011), lung and spleen (unpublished data), and to drive proliferation of recruited monocyte-derived cells (Jenkins et al., 2011). These studies did not reveal whether the actions of IL-4 were direct or indirect.

Akt signaling is required for CSF-1-mediated proliferation (Huynh et al., 2012; Irvine et al., 2006; Smith et al., 2000) and we have recently shown that intact Akt signaling is critically important for in situ MΦ proliferation in response to IL-4 (Ruckerl et al., 2012). IL-4 receptor (IL-4R) signaling however, does not effectively activate Akt in MΦ in vitro despite phosphorylating PKB (Heller et al., 2008), thus raising the possibility that IL-4 acts via CSF1R signaling to induce Akt-dependent MΦ proliferation. Indeed, many important parallels exist between IL-4 and CSF-1 activated MΦ. For example, both IL-4 and CSF-1 promote a suppressive and a pro-repair phenotype in MΦ (Alikhan et al., 2011). Further, the transcription factors c-Myc and KLF-4, are critical for both the 'alternative activation' state induced in MΦ by engagement of the IL-4R (Liao et al., 2011; Pello et al., 2011), and CSF-1-dependent proliferation that occurs in the absence of Maf B and c-Maf (Aziz et al., 2009). Thus, understanding the relationship between CSF-1 and IL-4 is important, not least because several groups have used CSF-1 to generate human 'M2' MΦ (Fleetwood et al., 2007; Martinez et al., 2006; Verreck et al., 2004), which are often considered highly parallel to alternatively activated MΦ driven by IL-4.

This study seeks to determine the contribution of CSF-1 to IL-4 driven MΦ proliferation and alternative activation. Alternatively activated MΦ are a distinguishing feature of inflammation driven by helminth infections and allergy but may also appear in cold-stressed adipose tissue (Karp and Murray, 2012; Nguyen et al., 2012), certain immunogenic tumors (DeNardo et al., 2009; Linde et al., 2012), and even the steady-state (Wu et al., 2011). Using direct delivery of IL-4 and Th2-biased infection models, we demonstrate that IL-4-mediated proliferation requires MΦ-intrinsic IL-4Rα signaling that is entirely independent of the CSF1R. However, these

studies revealed a significant contribution of IL-4Rα independent, CSF1R-dependent MΦ proliferation during nematode infection. We further demonstrate that IL-4Rα expression confers a major competitive advantage to MΦ, such that IL-4Rα^{+} cells rapidly outcompete those lacking receptor expression.

Results

IL-4 dependent proliferation does not require the CSF1R. We utilized delivery of IL-4c as a reductionist approach to investigate whether IL-4 acts via the CSF1R to drive expansion of resident serous cavity MΦ. Ki67 expression was used to determine the frequency of all F4/80^{High} MΦ in cycle, as described previously (Jenkins et al., 2011), while a 3hr BrdU pulse prior to necropsy or high level of Ki67 expression (Ki67^{High}) was used to indentify cells in S phase (Fig. S1A; (Landberg et al., 1990)). Intracellular staining for RELMα and/or Ym1 were used as markers of alternative activation. Consistent with the established role of CSF-1 in regulating steady state MΦ levels (Davies et al., 2013), proliferation observed in control PBS-treated mice was completely blocked by treatment with anti-CSF1R mAb (Fig. 1A). In contrast, neither elevated proliferation nor marker induction by IL-4c was affected by antibody treatment (Fig. 1A). The only influence of blocking CSF1R on IL-4c treatment was to reduce the final MΦ number (Fig. 1A). Daily oral gavage of GW2580, an inhibitor of the CSF1R tyrosine kinase, also had no effect on IL-4-induced MΦ proliferation or alternative activation (Fig. 1B). Furthermore, *Csf1r* gene expression was significantly reduced in FACS-purified peritoneal MΦ 24h after injection of IL-4c (Fig. 1C). As expected, because the ligand is cleared by receptor-mediated endocytosis (Hume and MacDonald, 2011), CSF1R blockade resulted in elevated levels of CSF-1 in the tissue and bloodstream (Fig. 1D), thereby confirming the effectiveness of the antibody. However, CSF-1 production was not increased in response to IL-4 (Fig. 1D). Thus, in the context of IL-4 delivery there was no evidence of CSF1R involvement in proliferation and alternative activation.

IL-4 driven proliferation requires MΦ-intrinsic IL-4Rα-signaling. We next addressed the possibility that IL-4 signals directly to MΦ to induce proliferation. We used *LysM^{cre}Il4ra$^{-/lox}$* mice to delete the IL-4Rα chain on myeloid cells including MΦ

and neutrophils (Herbert et al., 2004). Injection of IL-4c into *LysM*^{cre}*Il4ra*$^{-/lox}$ mice resulted in elevated proliferation of F4/80^{High} MΦ in the cavities as well as elevated frequencies of alternatively activated MΦ (Fig. 2A). Nevertheless, MΦ proliferation was lower in *LysM*^{cre}*Il4ra*$^{-/lox}$ mice than in *Il4ra*$^{-/lox}$ controls (pleural, $P < 0.01$, Fig. 2B; peritoneal, $P < 0.001$). Co-staining for RELMα and BrdU (Fig. 2B) revealed that RELMα^{+} MΦ from *LysM*^{cre}*Il4ra*$^{-/lox}$ mice underwent significantly greater levels of proliferation than RELMα^{-} cells. Because RELMα expression is a known marker of IL-4Rα engagement on MΦ (Jenkins and Allen, 2010) and LysM-Cre is relatively inefficient (Hume, 2011) the data suggest that IL-4-dependent proliferation predominantly occurs in the subset of MΦ that retain the IL-4R in *LysM*^{cre}*Il4ra*$^{-/lox}$ animals.

To confirm this conclusion, *Il4ra*$^{+/+}$*Cd45.1*$^{+}$*Cd45.2*$^{+}$ C57BL/6 mice were lethally irradiated and transplanted with a 50:50 mix of BM from *Il4ra*$^{+/+}$*Cd45.1*$^{+}$*Cd45.2*$^{+}$ and *Il4ra*$^{-/-}$*Cd45.2*$^{+/+}$ *Cd45.1*^{null} mice, so that cells derived from *Il4ra*$^{-/-}$ BM could be distinguished from WT by a lack of CD45.1 expression. Blood-borne monocytes (Fig. 2C) and other myeloid populations (data not shown) exhibited roughly equal proportions of CD45.1^{+} and CD45.1^{-} cells 8wk after reconstitution. This extends earlier data showing the key mediator of IL-4R signaling, STAT6, has no intrinsic role in steady-state proliferation or survival of hematopoietic stems cells despite their ubiquitous IL-4Rα^{+} expression (Bunting et al., 2004). Likewise, similar frequencies of *Il4ra*$^{+/+}$ and *Il4ra*$^{-/-}$ cells were detected in the resident F4/80^{High} pleural and peritoneal cavity MΦ populations in control mice treated with PBS (Fig. 2D & data not shown). By contrast, *Il4ra*$^{+/+}$ F4/80^{High} MΦ greatly out numbered *Il4ra*$^{-/-}$ cells in the pleural and peritoneal cavities of mice treated with IL-4c. Indeed, only the IL-4Rα^{+} population increased in number following treatment with IL-4c (Fig. 2D & data not shown), consistent with increased S phase BrdU^{+} cells (Fig. 2E) and Ki67^{+} cells (data not shown) being observed only in the CD45.1^{+} IL-4Rα^{+} cells. Notably, steady-state levels of proliferation in PBS-treated controls did not differ between *Il4ra*$^{+/+}$ and *Il4ra*$^{-/-}$ cells, suggesting IL-4 is only important in an inflammatory context. Intracellular staining for RELMα (data not shown) and Ym1 (Fig. 2E) in these experiments confirmed an absolute requirement for intrinsic IL-4Rα-signaling to up-

regulate production of these archetypal alternative activation markers under this reductionist condition.

Both IL-4Rα-dependent and independent pathways contribute to proliferation during nematode infection. The Th2 cytokines IL-4 and IL-13 can both signal via the IL-4Rα to drive alternative activation (Gordon and Martinez, 2010). In our previous study, nematode-associated increased MΦ proliferation was not entirely absent in *Il4*$^{-/-}$ mice (Jenkins et al., 2011) suggesting a possible contribution from IL-13. To assess the potential of IL-13 to induce proliferation mice were injected with IL-13 complexed with a neutralizing antibody (IL-13c). IL-13c led to significant ($P < 0.01$) MΦ proliferation, at a similar magnitude to IL-4c delivery (Fig. 3A), but as documented previously (Heller et al., 2008), IL-13 was somewhat less effective at stimulating RELMα production by MΦ. To determine whether IL-13 was responsible for the residual rise in proliferation observed in nematode-infected *Il4*$^{-/-}$ mice, we infected mice lacking the IL-4Rα chain (*Il4ra*$^{-/-}$). Proliferation and accumulation of pleural MΦ following *Ls* infection was significantly ($P < 0.001$) reduced in *Il4ra*$^{-/-}$ mice compared to WT controls (Fig. 3B) but to no greater extent than in the *Il4*$^{-/-}$ mice (Jenkins et al., 2011) suggesting no contribution of IL-13. By contrast, marker induction in MΦ was entirely dependent upon IL-4Rα signaling (Fig. 3B) and worm burdens did not significantly differ between strains at this stage of infection (data not shown). Hence, mechanisms independent of the IL-4Rα contribute to elevated MΦ self-renewal during nematode infection. Comparison of the kinetics of alternative activation and proliferation stimulated by IL-4c vs *Ls* infection revealed key differences; IL-4c induced marker expression in peritoneal and pleural MΦ prior to detectable proliferation (Fig. 3C and S1B), while during infection proliferation preceded marker expression (Fig. 3D). The data indicate that IL-4Rα-independent proliferation occurs early during infection with subsequent peak proliferation driven by IL-4.

Of note, proliferation induced by a single IL-4c dose subsided after 4d, whereas alternative activation markers were sustained (Fig. 3C and S1B). Following two sequential IL-4c doses at d0 and d2 proliferation remained evident at d4 (Fig. 1A). We therefore titrated the dose of IL-4c. As expected, proliferative activity required

high doses of IL-4, whereas induction of RELMα was maximal at the lowest dose tested (Fig. 3E). Thus, detection of alternative activation markers in the tissues is not synonymous with proliferation, as marker expression may only indicate prior or low-level exposure to IL-4.

IL-4 switches MΦ to CSF-1-independent proliferation. We used CSF1R blockade to assess the potential contribution of CSF1R-signaling to the IL-4Rα-independent proliferation that occurs during *Ls* infection. Mice were treated with anti-CSF1R mAb between d8 and 10 to coincide with the approximate onset of alternative activation (Fig. 3D) and when IL-4R-independent proliferation is detectable (Fig. 3B). CSF1R blockade led to a significant reduction in infection-induced proliferation of pleural MΦ (Fig. 4A), whereas alternative activation (Fig. 4A), Th2 responses, and worm burden (data not shown) were unaffected. However, the response in the infected group appeared bimodal, with 13 of 20 anti-CSF1R treated mice showing almost complete inhibition of proliferation (Fig. 4A; black squares), while the remaining animals were similar to controls (Fig. 4A; grey squares). The anti-CSF1R-treated infected animals in which high-level proliferation remained evident showed the highest frequencies of $Ym1^+$ MΦ (Fig. 4A; grey squares), and indeed the frequency of MΦ able to proliferate in the presence of anti-CSF1R correlated positively with $Ym1^+$ MΦ (Spearman r = 0.84, p<0.0001). The data suggest that as the strength of Th2 response and corresponding IL-4Rα-signaling increased, the dependence upon CSF1R-signaling for MΦ to proliferate and accumulate during tissue nematode infection declined. In other words, IL-4 can substitute for CSF-1.

CSF-1 is increased in the circulation and local lesions in many infections, chronic inflammation and malignancy (Chitu and Stanley, 2006; Hume and MacDonald, 2011). We therefore measured levels of cytokine in the pleural lavage fluid and serum. There was a modest increase in accumulation of CSF-1 in the pleural cavity of infected anti-CSF1R treated mice compared to naïve controls, but no increase in the serum (Fig. 4B). No correlation was found between the level of pleural CSF-1 and frequency of $BrdU^+$ MΦ in anti-CSF1R-treated infected mice (Spearman r = 0.1398, $P = 0.5565$), consistent with IL-4R-signalling controlling CSF-1-independent proliferation in these mice directly rather than via elevation of CSF-1.

IL-4Rα expression provides a competitive advantage to MΦ during nematode infection. We next infected *Il4ra*$^{+/+}$*Cd45.1*$^{+}$: *Il4ra*$^{-/-}$ *Cd45.1*^{null} mixed BM chimeric mice with *Ls* to investigate the relevance of MΦ-intrinsic IL-4Rα-signaling in a setting in which IL-4Rα-independent proliferation can occur. In contrast to the highly restricted response seen in these mice following IL-4c injection (Fig. 2D&E), increased proliferation of both *Il4ra*$^{+/+}$ and *Il4ra*$^{-/-}$ pleural F4/80^{High} MΦ was evident by d10 post-*Ls* infection (Fig. 5A). The frequency of cycling cells was however, significantly greater in the IL-4Rα^{+} population in all infected mice at this time ($P < 0.001$), and only in these cells did heightened proliferation remain evident at d16 (Fig. 5A). In contrast, production of Ym1 (Fig. 5A) and RELMα (data not shown) during infection was wholly dependent upon MΦ intrinsic IL-4Rα-signaling. Consistent with the pattern of proliferation, both *Il4ra*$^{+/+}$ and *Il4ra*$^{-/-}$ populations significantly increased in number in the pleural cavity by d10 post-infection ($P < 0.01$), yet by d16 the IL-4Rα^{-} MΦ, although still elevated in number ($P < 0.05$), were significantly outnumbered by the IL-4Rα^{+} cells (Fig. 5B; $P < 0.05$). The selective-advantage provided by the IL-4Rα was only observed in the F4/80^{High} MΦ population and not other myeloid cells (Fig. 5C). Thus, while confirming the existence of an IL-4Rα-independent pathway of proliferation, these data show that direct IL-4Rα-signaling to MΦ conveys a competitive advantage during infection at least in part by enhancing entry into cell-cycle. These findings explain the emergence of RELMα^{+} pleural MΦ in MΦ-specific IL-4Rα-deficient *LysM*^{cre}*Il4ra*$^{-/lox}$ mice during the later phase of *Ls* infection (Fig. 5D). Indeed, by day 60 post-infection, RELMα and YM1 expression by MΦ is indistinguishable between WT and *LysM*^{cre}*Il4ra*$^{-/lox}$ mice (data not shown). IL-4Rα expression on MΦ in the *LysM*^{cre}*Il4ra*$^{-/lox}$ mice was confirmed by surface staining (Fig. 5D). Thus, IL-4Rα expression can give MΦ a competitive advantage during a chronic Th2-inflammatory setting such as helminth infection.

Proliferation during infection requires adaptive immunity and is localized to the infection site. We have previously established using *Rag1*$^{-/-}$ mice that IL-4 driven MΦ proliferation *per se* does not require adaptive immunity (Jenkins et al., 2011). In the context of chronic nematode infection however, MΦ accumulation requires Th2 cells and MHC class II (Loke et al., 2007). We thus assessed the requirement for

adaptive immunity in MΦ proliferation during infection. There was a dramatic reduction in the number of F4/80^{+} MΦ in nematode-infected *Rag1*$^{-/-}$ mice compared to WT controls, matched by a complete failure of the MΦ to divide or up-regulate alternative activation markers (Fig. 5E). Consistent with a need for cognate antigen specific interaction, proliferation and alternative activation were localized to the site of parasite infection in WT animals, with significantly ($P < 0.05$) elevated responses observed in the pleural but not the peritoneal cavity of infected mice (Fig. 5F).

IL-4 dependent MΦ proliferation, alternative activation and competitive advantage are features of intestinal nematode infection. Oral infection of BALB/c mice with the gastrointestinal (GI) nematode *Heligmosomoides polygyrus bakeri* (*Hp*) leads to invasion of the submucosa of the duodenum where the worms undergo developmental maturation. Despite restriction of the worms to the GI tract, there is systemic dissemination of Th2 cells with selectivity for the peritoneal cavity (Mohrs et al., 2005). In *Hp* infected mice, there was a striking increase in proliferation of F4/80^{High} resident MΦ by day 7 post-infection in the peritoneal (Fig. 6A) but not the pleural cavity (data not shown) consistent with the localized MΦ proliferation observed in our *Ls* model. Infection led to a 2 to 3-fold increase in cells in the peritoneal lavage, exclusively within the F4/80^{High} MΦ population. As expected for a Th2 setting, these MΦ expressed RELMα and Ym1 (Fig. 6A). As in the *Ls* model, *Il4*$^{-/-}$ mice had a reduced response, although a significant increase in BrdU^{+} ($P < 0.001$), Ki67^{+} ($P < 0.001$) and total MΦ ($P < 0.01$) remained (Fig. 6B). A minor population of Ym1^{+} MΦ were also detected in infected *Il4*$^{-/-}$ mice suggesting a limited influence of IL-13 (Fig. 6B). Blockade of CSF1R signaling demonstrated a CSF1R-dependent component to the proliferative but not the alternative activation response (Fig. 6C), and thus as in the *Ls* model both CSF1R and IL-4Rα signaling also contribute to MΦ proliferation in this model. We also re-examined the relative importance of cell autonomous IL-4R signaling in the *Hp* model. The majority of F4/80^{High} MΦ, but not other myeloid cell populations, were IL-4Rα^{+} by d14 post-infection of *Il4ra*$^{+/+}$*Cd45.1*$^{+}$: *Il4ra*$^{-/-}$ *Cd45.1*^{null} mixed BM chimeric mice, despite earlier accumulation of both IL-4Rα^{+} and IL-4Rα^{-} cells (Fig. 6D). This competitive advantage was confirmed using *LysM*^{cre}*Il4ra*$^{-/lox}$ mice infected with *Hp*, in which the proportion of RELMα positive cells increased from 4% in naïve mice (data not

shown) to 25% at day 14 and 70% by day 28 (Fig. 6E), by which point more than 50% of the MΦ expressed IL-4Rα detectable by flow cytometry (data not shown). Infection with a GI nematode thus led to a MΦ response in the peritoneal cavity that mirrored the pleural cavity during infection with the filarial worm *Ls*. In both models CSF1R and IL-4Rα contributed independently to proliferation.

Differing consequences of CSF-1 vs IL-4 induced inflammation. Since both IL-4 and CSF-1 can induce local MΦ proliferation, we sought to compare the MΦ elicited by the two stimuli. To assess the contribution of CSF-1 to cellular dynamics in the serous cavity, we used a new reagent, Fc-CSF-1 designed for stable in vivo delivery of CSF-1. We compared Fc-CSF-1 to IL-4c at similar molar doses that induced maximal levels of proliferation with both reagents (≥80% $Ki67^+$ by 48hr, data not shown). Despite near identical levels of MΦ proliferation at 24hr, only IL-4c induced RELMα (Fig. 7A) or Ym1 (data not shown) production. Furthermore, Fc-CSF-1 induced the recruitment of inflammatory cells including neutrophils and $Ly\text{-}6C^+$ monocytes (Fig. 7B), consistent with its recently described ability to drive pro-inflammatory chemokine production (Tagliani et al., 2011) and acute monocytopenia (Ulich et al., 1990). In striking contrast, no inflammatory recruitment was seen with IL-4c, consistent with the ability of IL-4 to actively down-regulate pro-inflammatory chemokines (Thomas et al., 2012). Thus although CSF-1 and IL-4 both induce MΦ proliferation in the tissues, they have otherwise markedly different consequences. Additionally, these data demonstrate that elevated CSF-1 signaling is sufficient to stimulate heightened proliferation (Fig. 7A) and accumulation (data not shown) of resident MΦ in vivo without need for additional signals that occur during infection/inflammation, and provide some explanation for the elevated peritoneal MΦ numbers seen in the original studies of systemic CSF-1 treatment of mice (Hume et al., 1988).

Discussion

Previous studies demonstrated the requirement for IL-4 to achieve maximal proliferation of MΦ during nematode infection and an absolute requirement for the IL-4Rα for MΦ proliferation following IL-4c delivery (Jenkins et al., 2011). Our working hypothesis was that IL-4 acted indirectly via an intermediate cell, to

stimulate production of a MΦ mitogenic factor, such as CSF-1, similar to the process by which a Vitamin D3 analogue acts on keratinocytes to stimulate Langerhans cell proliferation (Chorro et al., 2009). This hypothesis was supported by our preliminary data in which IL-4 driven proliferation was observed in mice apparently lacking IL-4Rα on MΦ. However, using mixed BM chimeric mice we demonstrate that MΦ intrinsic IL-4Rα signaling is required for MΦ proliferation in response to endogenous or exogenous IL-4. Furthermore, IL-4 mediated proliferation was entirely independent of CSF1R-signalling, in contrast to the homeostatic proliferation of cavity resident MΦ, which is completely dependent upon CSF-1 (Fig. 1A,1B&4A)(Davies et al., 2013). Treatment with IL-4c did not increase production of CSF-1 in either serum or tissues, consistent with an intrinsic and CSF-1-independent effect of IL-4 on MΦ. Thus, it would appear that IL-4Rα signaling to MΦ allows their substantial outgrowth above normal tissue levels at least in part by switching them to a CSF-1-independent program of proliferation.

Nevertheless, IL-4R^{+} MΦ remain reliant upon CSF-1 for survival following IL-4-driven expansion, as indicated by the reduced numbers observed following CSF1R blockade. Seemingly at odds with such a requirement, we found that IL-4 treatment was accompanied by a sharp down-regulation in MΦ transcription of the CSF1R. However, lower levels of CSF1R signaling are required for MΦ survival than are needed for their proliferation (Tushinski et al., 1982). CSF-1 is likely present in the steady-state serous cavities in greater abundance than required for MΦ survival given the evident homeostatic CSF-1-dependent proliferation in these sites (Fig. 1&3)(Davies et al., 2013). We suggest that IL-4-mediated down-regulation of CSF1R reduces local CSF-1 consumption by individual cells thereby maintaining sufficient tissue CSF-1 levels to allow survival of the expanding MΦ population. Such a model would explain how the basal levels of proliferation and total number of IL-4Rα^{-} MΦ in mixed BM chimeras appeared to be maintained at near normal steady-state levels following treatment with IL-4c (Fig. 2E) despite the large out-growth of IL-4Rα^{+} cells and without corresponding increase in CSF-1 production (Fig. 1D). Together, our data suggest that IL-4 and CSF-1 are entirely distinct in terms of proliferation although CSF-1 is still critical for survival in the context of IL-4 expansion.

During nematode infection, our data suggests that CSF-1 plays an early role in MΦ proliferation but is superseded by IL-4 presumably upon entry of Th2 cells. Supporting this, CSF1R blockade during infection almost completely inhibited proliferation in all WT animals except those exhibiting the highest levels of IL-4 exposure as indicated by the percent of cells expressing alternative activation markers (Fig. 4A). Furthermore, time course analysis during infection demonstrated that proliferation occurred before, but only peaked after, the onset of alternative activation (Fig. 3D), while more sustained and higher proliferation was achieved by IL-4Rα^{+} than IL-4Rα^{-} cells in infected mixed BM chimeric mice (Fig. 5A). Lastly, the restriction of proliferation and MΦ accumulation to the infection site, and the absence any such response in *Rag1*$^{-/-}$ animals (Fig. 5E & F) mirrors our previous findings that MΦ fail to accumulate in a related nematode infection in the absence of Th2 cells (Loke et al., 2007). IL-4 may also contribute to elevated tissue MΦ density during infection through additional cell-intrinsic mechanisms, for example, by reducing reliance on local glucose levels (Vats et al., 2006), inhibiting migration from the tissue (Thomas et al., 2012), or protecting against apoptosis, as occurs in other leukocytes (Wurster et al., 2002). While the mixed *Il4ra*$^{+/+}$*: Il4ra*$^{-/-}$ BM mice do not reflect the natural distribution of IL-4R expression in vivo, they are critically important for understanding how cell-intrinsic IL-4R-signalling augments MΦ numbers during nematode infection. Furthermore, the data generated using these mice may be relevant to circumstances in which differential IL-4R expression does occur (Wermeling et al., 2013).

RELMα and Ym1 were used here as surrogate markers of IL-4R experienced MΦ. Elsewhere, Ym1 expression has been documented in MΦ from *LysM*^{cre}*Il4ra*$^{-/lox}$ mice in the liver granulomas surrounding schistosome eggs and peritoneal cavity following injection of schistosome eggs (Dewals et al., 2010). Because Ym1 expression is reduced significantly by in vivo IL-10 blockage it was concluded that IL-10 induces MΦ Ym1 expression in these settings independently of IL-4 (Dewals et al., 2010). However, we observed a large proportion of serous cavity MΦ in *LysM*^{cre}*Il4ra*$^{-/lox}$ mice expressing Ym1 and RELMα in response to IL-4c injection and during infection with *Ls* or *Hp*, with co-staining confirming IL-4Rα expression. Moreover, expression of both Ym1 and RELMα was exclusively restricted to IL-4Rα^{+} MΦ in IL-4-treated

or nematode infected mixed BM chimeric mice despite abundant IL-10 detectable in the pleural lavage fluid during infection (data not shown). It would seem that the selective advantage of IL-4Rα expression leads to accrual of a minor non-gene-deleted population, which could account for the $Ym1^{+}$ cells observed in $LysM^{cre}Il4ra^{-/lox}$ mice during schistosome infection (Dewals et al., 2010). Alternatively, MΦ elicited by schistosome eggs may differ qualitatively from those found during nematode infection and IL-4c injection, being capable of Ym1 production in response to IL-10. In this respect, schistosome eggs elicit CCR2-dependent inflammatory MΦ (Chensue et al., 1996; Lu et al., 1998), contrasting with the resident-derived cells in our systems (Jenkins et al., 2011). Furthermore, $Il4ra^{-/-}$ and $LysM^{cre}Il4ra^{-/lox}$ mice show no defect in overall MΦ numbers elicited to schistosome granulomas (Dewals et al., 2010), perhaps due to the pro-inflammatory nature of the eggs. Therefore, the balance of proliferation vs recruitment in Th2 settings almost certainly depends upon integration of multiple inflammatory signals. Of relevance, variation of IL-4c dose and delivery timing suggested that proliferation may only be apparent in environments in which critical IL-4 thresholds are sustained.

Steady-state proliferation in naïve animals was not influenced by IL-4Rα signaling, either in mixed BM chimeric mice, $LysM^{cre}Il4ra^{-/lox}$ mice or in global IL-4Rα-deficient animals demonstrating that IL-4 mediates density of cavity MΦ only under conditions of inflammation and not homeostasis. IL-4Rα signaling also had little or no bearing on the wholly CSF-1-dependent elevated proliferation of resident peritoneal MΦ that occurs during resolution of microbial-induced peritonitis (Davies et al., 2013). In this process however, proliferation acts simply to restore the MΦ population to its original level following depletion during the acute stage of inflammation (Davies et al., 2011) and is therefore akin to homeostatic maintenance rather than an inflammatory process. In keeping with this, the levels of CSF-1 did not differ between naïve and inflammatory challenged mice in these studies (Davies et al., 2013). Elevated levels of circulating CSF-1 do occur in many disease states and administration of CSF-1 can greatly increase tissue MΦ numbers in rodents and primates (Hume and MacDonald, 2011), but it is unclear if this increase results from the outgrowth of resident MΦ or recruitment of new monocyte-derived cells. Using a recombinant Fc-CSF-1 fusion protein we demonstrate that CSF-1 efficiently

stimulates proliferation of resident peritoneal MΦ (Fig. 7A). Furthermore, during nematode infection, we detected an approximate doubling in the number of IL-4Rα-deficient MΦ in mixed BM chimeras (Fig. 5) and in global *Il4ra*$^{-/-}$ mice (Fig. 3B), mirroring the two-fold increase in local CSF-1 production (Fig. 5E). Elevated CSF-1 can therefore act during an inflammatory episode to increase local numbers of resident tissue MΦ, and could play a more significant role in expansion of resident MΦ in pathologies in which much higher CSF-1 levels are observed (Hamilton, 2008).

Although both IL-4 and CSF-1 elicited proliferation of resident MΦ, they differed fundamentally in other actions. In particular, injection of Fc-CSF-1 also induced recruitment of Ly6C^{+} monocytes and neutrophils, consistent with reports elsewhere (Lenda et al., 2003; Tagliani et al., 2011), suggesting elevated CSF-1 secretion may act as an emergency stopgap to rapidly fill the tissue MΦ compartment. In contrast, we saw no evidence of increased recruitment of inflammatory cells following IL-4c administration and previously observed recruitment of only low numbers during the early stages of *Ls* infection despite the large increase in resident tissue MΦ (Jenkins et al., 2011). CSF1R signaling directly induces production of CCR2 ligands by tissue MΦ in order to stimulate recruitment of Ly-6C^{+} monocytes (Tagliani et al., 2011), while IL-4 down-regulates MΦ production of CCL2, CCL7, and CCL3, during tissue nematode infection (Thomas et al., 2012). While the finding that IL-4 mediated proliferation is CSF1R-independent was at first unexpected, our data suggests that this mechanism may have developed as an alternative to a CSF-1 pathway in order to increase numbers of resident MΦ without co-incident increase in monocyte recruitment. This could be seen as an additional tissue protective function of IL-4 beyond induction of the immunoregulatory and pro-wound repair phenotype associated with alternative activation (Murray and Wynn, 2011).

In summary, the impact of IL-4 during infections is likely two-fold; it increases numbers without need for recruitment, while in the presence of recruitment it insures a non-inflammatory environment by switching MΦ to an alternatively activated phenotype. Thus, the numerical advantage provided by MΦ IL-4Rα expression combined with the anti-inflammatory chemokine profile, and alternative activation

state ultimately leads to the development of a non-inflammatory environment to contain worm infection and repair tissue regardless of MΦ source.

Acknowledgements

The authors thank A. Fulton, S. Afrough, S. McGarvie and E. Slattery for technical assistance, and Dr. P. Taylor for critical reading of the manuscript. This work was funded by the Medical Research Council UK (G0600818 & MR/K01207X/1 to J.E.A.), with additional support from the Welcome Trust (strategic award for Centre for Immunity, Infection and Evolution; 082611/Z/07/Z , Ph.D studentship to G.D.T. and grants to R.M.M.). F.B. is a South African Research Chair holder supported by the National Research Foundation (South Africa) and South African Medical Research Council. D.A.H was supported by an Institute Strategic Programme Grant to The Roslin Institute from the BBSRC (project grant BB/H012559/1). The Fc-CSF-1 reagent is the subject of UK patent Application GB1303537.1. The authors have no additional conflicting financial interests.

Material and Methods

Mice

BALB/c *Il4*$^{-/-}$ (Noben-Trauth et al., 1996), *Il4ra*$^{-/-}$, *LysM*^{cre}*Il4ra*$^{-/lox}$, and *Il4ra*$^{-/lox}$ mice (Herbert et al., 2004) and C57BL/6 *Il4ra*$^{-/-}$ and *Rag1*$^{-/-}$ mice and wild-type controls were bred and maintained in specific-pathogen free facilities at the University of Edinburgh. All experiments were permitted under a Project License granted by the Home Office UK and were approved by the University of Edinburgh Ethical Review Process. Experimental mice were age and sex matched. C57BL/6 *Il4ra*$^{-/-}$ mice were generated by back-crossing from the BALB/c *Il4ra*$^{-/-}$ strain a minimum of '9' times. Competitive mixed BM chimeric mice were created by lethally irradiating C57BL/6 *Cd45.1*$^{+}$ *Cd45.2*$^{+}$ mice with 11.5 Gy γ radiation administered in two doses approximately 3h apart followed by i.v. injection of with 5 x 10^6 BM cells depleted of mature T cells using CD90 microbeads (Miltenyi Biotec) and comprised of a 1:1 mix of cells from C57BL/6 *Cd45.2*$^{+/+}$ *Il4ra*$^{-/-}$ mice and C57BL/6 *Cd45.1*$^{+}$ *Cd45.2*$^{+}$ mice. Chimeric animals were left for at least 8 wk before further experimental manipulation.

Parasites and reagents

Hp and *Ls* life cycles were maintained and infective third-stage larvae (L3) obtained as described elsewhere (Behnke and Wakelin, 1977; Le Goff et al., 2002). Mice were infected with 200 *Hp* L3 by oral gavage or 25 *Ls* L3 by s.c. injection. IL-4/anti-IL-4 mAb (IL-4c) were prepared as described previously (Finkelman et al., 1993) and unless stated otherwise, mice injected i.p. with 5μg of recombinant IL-4 (Peprotech; 13.5 kDa) complexed to 25μg 11B11 (BioXcell) or 100μl PBS vehicle control on d0 and 2, and peritoneal and pleural exudate cells harvested on d4. IL-13/anti-IL-13 complexes were similarly prepared using 5μg recombinant IL-13 (Peprotech; 12.3 kDa) complexed to 25μg eBio13A (eBioscience). Fc-CSF-1 is a fusion protein of pig CSF-1 with the Fc region of pig IgG1A (43.82 kDa total) that was produced using mammalian cell line expression by Zoetis for D. Hume (UK patent Application GB1303537.1). CSF-1 was conjugated to Fc for increased stability in vivo. Extensive studies in mice and pigs reveal that pig CSF-1 is equally active in mice (Gow et al., 2012). The presence of endotoxin-like activity in Fc-CSF-1 was tested in murine bone marrow-derived macrophages. There was no detectable induction of the LPS-responsive TNF-α gene under conditions in which LPS induced the gene more than

1000-fold. Mice were injected with 20μg i.p. Fc-CSF-1 in PBS. Where specified, mice were given 1mg BrdU i.p. 3h before experimental end-point.

Isolation of cells from the peritoneal and pleural cavity

Mice were sacrificed by exsanguination via the brachial artery under terminal anesthesia. Following sacrifice, pleural or peritoneal cavity exudate cells were obtained by washing of the cavity with lavage media comprised of RPMI 1640 containing 2mM L-glutamine, 200U/ml Penicillin, 100 μg / ml Streptomycin and 2 mM EDTA (Invitrogen). The first 2 or 3ml of lavage wash supernatant from the pleural or peritoneal cavities, respectively, was frozen prior to analysis by ELSIA. Worm burden in the pleural lavage fluid of *Ls* infected mice was determined by counting under a Leica MZ9 stereo-microscope. Erythrocytes were removed by incubating with red blood cell lysis buffer. Cellular content of the cavities and organs was assessed by cell counting using a Casy TT cell counter (Roche) in combination with multi-color flow-cytometry.

Flow cytometry

Equal numbers of cells or 20 μl of blood were stained for each sample. Blood samples were mixed and washed with Hank's buffered saline solution containing 2mM EDTA (Invitrogen). Cells were stained with LIVE/DEAD® (Invitrogen). All samples were then blocked with 5 μg/ml anti-CD16/32 (2.4G2; produced in-house) and heat-inactivated normal mouse serum (1:20) in FACS buffer (0.5% BSA, 2mM EDTA in Dulbeccos PBS) before surface staining on ice with antibodies to F4/80 (BM8), Siglec-F (E50-2440), Ly-6C (AL-21 or HK1.4), Gr-1 (RB6-8C5), CD11b (M1/70), CD11c (N418), MHCII (M5/114.15.2), CD19 (eBio1D3), CD4 (GK1.5), CD3 (17A2), CD115 (AFS98), IL-4Rα (mIL4R-M1), CD45.1 (A20) or CD45.2 (104) (eBioscience, or BD Europe). Erythrocytes in blood samples were lysed using FACSlyse solution (BD Europe).

Detection of intracellular RELMα, Ym1, Ki67 and BrdU was performed directly *ex vivo*. Cells were stained for surface markers then fixed and permeabilized using FoxP3 staining buffer set (eBioscience). For BrdU staining, cells were incubated first with or without DNase for 30 mins at 37^{o}C. Cells were then stained with biotinylated

goat anti-Ym1 (R & D Systems), purified polyclonal rabbit anti-RELMα (Peprotech EC, London, UK) or directly labeled monoclonal antibodies to Ki67 (B57) or anti-BrdU (B44 or Bu20a) (BD Europe or Biolegend) followed by Zenon anti-rabbit reagent (Invitrogen) or Streptavidin-conjugated fluorochromes (Biolegend). Expression of Ym1, RELMα and Ki67 was determined relative to appropriate polyclonal or monoclonal isotype control, whereas incorporation of BrdU was determined relative to staining on non-DNase treated cells. Analysis of proliferation and alternative activation was performed on single live cells, determined using LIVE/DEAD® and forward-scatter width (FSC-W) vs forward-scatter area (FSC-A), respectively, and subsequently gated on $CD19^-$ cells to remove B-cell:MΦ doublets. Analysis for calculation of total $F4/80^{High}$ MΦ was performed on all cells. Samples were acquired using FACS LSR II or FACS Canto II using BD FACSDiva software (BD Europe) and analyzed with FlowJo v9 software (Tree Star, Inc.).

Analysis of MΦ from competitive mixed BM chimeras

MΦ derived from *Cd45.1*$^+$ *Il4ra*$^{+/+}$ BM appeared to have a greater tendency to form doublets with $CD19^+$ B cells following injection of IL-4c than cells derived from *Cd45.1*$^-$ *Il4ra*$^{-/-}$ BM, as judged by the high level of F4/80 expression on B cell:MΦ doublets (Fig. S2A), a marker which is know to be up-regulated by IL-4R-signaling (Jenkins et al., 2011). If doublets were excluded from analysis, such bias in doublet formation would distort the ratio of WT to *Il4ra*$^{-/-}$ MΦ. Thus, cells were treated for 5 minutes with Accumax cell aggregate dissociation medium (eBioscience) immediately prior to fixation, and population frequency analysis performed without a single cell gate applied. To further prevent bias induced by the few remaining doublets, the gate for $CD45.1^+$ $CD45.2^+$ cells was set to exclude events that deviated from the expected linear relationship of CD45.1 and CD45.2 on this population (R1 Fig. S2B). Analysis of proliferation and alternative activation in these experiments was performed on $CD19^-$ $F4/80^{High}$ MΦ gated on single cells, using FSC-W vs FSC-A, to minimize the potential for false positives (R2 Fig. S2B). Due to a minor bias towards more WT than *Il4ra*$^{-/-}$ pleural MΦ in naïve chimeras, 1-way ANOVA was used to analyze differences in cell numbers following infection, whereas paired statistical tests were used to analyze rates of proliferation and alternative activation, to better account for the variation in overall level of proliferation between mice.

CSF1R studies

Mice were injected i.p. with 0.5 mg anti-CSF1R mAb (Clone AFS98), purified rat IgG control antibody, or PBS vehicle control either concurrent with IL-4c injections or on d8 post-*Ls* infection or d6 post-*Hp* infection. AFS98 mAb and purified rat IgG control were produced in house from cultured hybridoma cells or from naïve rat serum respectively. The c-fms kinase inhibitor GW2580 (Conway et al., 2005) (LC Laboratories) was suspended in 0.5% hydroxypropylmethylcellulose and 0.1% Tween20 using a Teflon glass homogenizer. Diluent control or 160 mg / kg GW2580 were administered daily by oral gavage from 1h before initial dose of IL-4c on d0, to 5h before mice were culled on d3. Previous pharmacokinetic analysis has shown this daily dose regime is as effective as twice daily administration of 80 mg / kg and maintains a serum concentration of the drug over 24h above that estimated to achieve therapeutic effect (Priceman et al., 2010). Analysis of CSF-1 in brachial arterial blood and pleural lavage fluid was performed as per manufacturers instruction (Peprotech EC).

MΦ purification and gene expression

Gene expression analysis on MΦ from IL-4c or PBS treated mice was performed on mRNA for which we have previously published data (Ruckerl et al., 2012). Briefly, 24h after treatment of mice with PBS or IL-4c peritoneal MΦ were sorted using a FACSAria cell sorter (BD Biosciences) according to their expression of $F4/80^{+}$, Siglec-F^{-}, $CD11b^{+}$, $CD11c^{-}$, $B220^{-}$, $CD3^{-}$ to purities above 90%. Total RNA was then isolated using the miRNEasy-kit (Qiagen) according to manufacturers instructions, measured using a NanoDrop (Thermo Scientific) and converted to cDNA with BioScript™ Reverse Transcriptase (Bioline) and $p(dT)_{15}$ Primers (Roche Applied Science). Expression levels were quantified using LightCycler® 480 SYBR Green I Master (Roche Applied Science), with measurements performed on a Lightcycler® 480 (Roche Applied Science). Expression of *Csf1r* (5'-CGAGGGAGACTCCAGCTACA-3' & 5'-GACTGGAGAAGCCACTGTCC-3') was normalized against *Gapdh* (5'-ATGACATCAAGAAGGTGGTG-3' & 5'-CATACCAGGAAATGAGCTTG-3').

Statistics

Data was log-transformed to achieve normal distribution and equal variance where required and then tested using 1-way ANOVA, or *t* test. Where equal variance or normal distribution was not achieved, Kruskal Wallace, or Spearman correlation was used. Paired *t* test was used to determine differences between proliferation and alternative activation of $CD45.1^+$ and $CD45.1^-$ MΦ obtained from *Ls*-infected competitive mixed BM chimeric mice. Statistics were performed using Prism 5 (GraphPad Software). Each data point represents one animal, with horizontal bars indicate mean values unless otherwise specified.

Online supplementary material. Fig. S1A shows that MΦ in S phase express the highest levels of Ki67, such that gating on $Ki67^{High}$ cells provides an accurate estimate of their frequency. Fig. S1B provides representative flow cytograms of Ki67, RELMα and Ym1 staining on peritoneal and pleural MΦ at various time after IL-4c injection. Fig. S2 shows the gating strategy used to determine frequency of MΦ subsets from competitive mixed BM chimera experiments.

References

Ajami, B., J.L. Bennett, C. Krieger, K.M. McNagny, and F.M. Rossi. 2011. Infiltrating monocytes trigger EAE progression, but do not contribute to the resident microglia pool. *Nat Neurosci*. 14:1142-1149.

Ajami, B., J.L. Bennett, C. Krieger, W. Tetzlaff, and F.M. Rossi. 2007. Local self-renewal can sustain CNS microglia maintenance and function throughout adult life. *Nat Neurosci*. 10:1538-1543.

Alikhan, M.A., C.V. Jones, T.M. Williams, A.G. Beckhouse, A.L. Fletcher, M.M. Kett, S. Sakkal, C.S. Samuel, R.G. Ramsay, J.A. Deane, C.A. Wells, M.H. Little, D.A. Hume, and S.D. Ricardo. 2011. Colony-stimulating factor-1 promotes kidney growth and repair via alteration of macrophage responses. *The American journal of pathology*. 179:1243-1256.

Aziz, A., E. Soucie, S. Sarrazin, and M.H. Sieweke. 2009. MafB/c-Maf deficiency enables self-renewal of differentiated functional macrophages. *Science*. 326:867-871.

Behnke, J.M., and D. Wakelin. 1977. Nematospiroides dubius: stimulation of acquired immunity in inbred strains of mice. *J Helminthol*. 51:167-176.

Bunting, K.D., W.M. Yu, H.L. Bradley, E. Haviernikova, A.E. Kelly-Welch, A.D. Keegan, and C.K. Qu. 2004. Increased numbers of committed myeloid progenitors but not primitive hematopoietic stem/progenitors in mice lacking STAT6 expression. *Journal of leukocyte biology*. 76:484-490.

Chensue, S.W., K.S. Warmington, J.H. Ruth, P.S. Sanghi, P. Lincoln, and S.L. Kunkel. 1996. Role of monocyte chemoattractant protein-1 (MCP-1) in Th1 (mycobacterial) and Th2 (schistosomal) antigen-induced granuloma formation: relationship to local inflammation, Th cell expression, and IL-12 production. *J Immunol*. 157:4602-4608.

Chitu, V., and E.R. Stanley. 2006. Colony-stimulating factor-1 in immunity and inflammation. *Current opinion in immunology*. 18:39-48.

Chorro, L., A. Sarde, M. Li, K.J. Woollard, P. Chambon, B. Malissen, A. Kissenpfennig, J.B. Barbaroux, R. Groves, and F. Geissmann. 2009. Langerhans cell (LC) proliferation mediates neonatal development, homeostasis, and inflammation-associated expansion of the epidermal LC network. *The Journal of experimental medicine*. 206:3089-3100.

Conway, J.G., B. McDonald, J. Parham, B. Keith, D.W. Rusnak, E. Shaw, M. Jansen, P. Lin, A. Payne, R.M. Crosby, J.H. Johnson, L. Frick, M.H. Lin, S. Depee, S. Tadepalli, B. Votta, I. James, K. Fuller, T.J. Chambers, F.C. Kull, S.D. Chamberlain, and J.T. Hutchins. 2005. Inhibition of colony-stimulating-factor-1 signaling in vivo with the orally bioavailable cFMS kinase inhibitor GW2580. *Proceedings of the National Academy of Sciences of the United States of America*. 102:16078-16083.

Dai, X.M., G.R. Ryan, A.J. Hapel, M.G. Dominguez, R.G. Russell, S. Kapp, V. Sylvestre, and E.R. Stanley. 2002. Targeted disruption of the mouse colony-stimulating factor 1 receptor gene results in osteopetrosis, mononuclear phagocyte deficiency, increased primitive progenitor cell frequencies, and reproductive defects. *Blood*. 99:111-120.

Davies, L.C., M. Rosas, S.J. Jenkins, C.T. Liao, M.J. Scurr, F. Brombacher, D.J. Fraser, J.E. Allen, S.A. Jones, and P.R. Taylor. 2013. Distinct bone marrow-derived

and tissue-resident macrophage lineages proliferate at key stages during inflammation. *Nat Commun*. 4:1886.
Davies, L.C., M. Rosas, P.J. Smith, D.J. Fraser, S.A. Jones, and P.R. Taylor. 2011. A quantifiable proliferative burst of tissue macrophages restores homeostatic macrophage populations after acute inflammation. *European journal of immunology*. 41:2155-2164.
DeNardo, D.G., J.B. Barreto, P. Andreu, L. Vasquez, D. Tawfik, N. Kolhatkar, and L.M. Coussens. 2009. CD4(+) T cells regulate pulmonary metastasis of mammary carcinomas by enhancing protumor properties of macrophages. *Cancer Cell*. 16:91-102.
Dewals, B.G., R.G. Marillier, J.C. Hoving, M. Leeto, A. Schwegmann, and F. Brombacher. 2010. IL-4Ralpha-independent expression of mannose receptor and Ym1 by macrophages depends on their IL-10 responsiveness. *PLoS Negl Trop Dis*. 4:e689.
Finkelman, F.D., K.B. Madden, S.C. Morris, J.M. Holmes, N. Boiani, I.M. Katona, and C.R. Maliszewski. 1993. Anti-cytokine antibodies as carrier proteins. Prolongation of in vivo effects of exogenous cytokines by injection of cytokine-anti-cytokine antibody complexes. *J Immunol*. 151:1235-1244.
Fleetwood, A.J., T. Lawrence, J.A. Hamilton, and A.D. Cook. 2007. Granulocyte-macrophage colony-stimulating factor (CSF) and macrophage CSF-dependent macrophage phenotypes display differences in cytokine profiles and transcription factor activities: implications for CSF blockade in inflammation. *J Immunol*. 178:5245-5252.
Gordon, S., and F.O. Martinez. 2010. Alternative activation of macrophages: mechanism and functions. *Immunity*. 32:593-604.
Gow, D.J., V. Garceau, R. Kapetanovic, D.P. Sester, G.J. Fici, J.A. Shelly, T.L. Wilson, and D.A. Hume. 2012. Cloning and expression of porcine Colony Stimulating Factor-1 (CSF-1) and Colony Stimulating Factor-1 Receptor (CSF-1R) and analysis of the species specificity of stimulation by CSF-1 and Interleukin 34. *Cytokine*. 60:793-805.
Hamilton, J.A. 2008. Colony-stimulating factors in inflammation and autoimmunity. *Nature reviews. Immunology*. 8:533-544.
Hashimoto, D., A. Chow, C. Noizat, P. Teo, M.B. Beasley, M. Leboeuf, C.D. Becker, P. See, J. Price, D. Lucas, M. Greter, A. Mortha, S.W. Boyer, E.C. Forsberg, M. Tanaka, N. van Rooijen, A. Garcia-Sastre, E.R. Stanley, F. Ginhoux, P.S. Frenette, and M. Merad. 2013. Tissue-Resident Macrophages Self-Maintain Locally throughout Adult Life with Minimal Contribution from Circulating Monocytes. *Immunity*. 38:792-804.
Heller, N.M., X. Qi, I.S. Junttila, K.A. Shirey, S.N. Vogel, W.E. Paul, and A.D. Keegan. 2008. Type I IL-4Rs selectively activate IRS-2 to induce target gene expression in macrophages. *Sci Signal*. 1:ra17.
Herbert, D.R., C. Holscher, M. Mohrs, B. Arendse, A. Schwegmann, M. Radwanska, M. Leeto, R. Kirsch, P. Hall, H. Mossmann, B. Claussen, I. Forster, and F. Brombacher. 2004. Alternative macrophage activation is essential for survival during schistosomiasis and downmodulates T helper 1 responses and immunopathology. *Immunity*. 20:623-635.
Hume, D.A. 2011. Applications of myeloid-specific promoters in transgenic mice support in vivo imaging and functional genomics but do not support the

concept of distinct macrophage and dendritic cell lineages or roles in immunity. *Journal of leukocyte biology*. 89:525-538.
Hume, D.A., and K.P. MacDonald. 2011. Therapeutic applications of macrophage colony-stimulating factor-1 (CSF-1) and antagonists of CSF-1 receptor (CSF-1R) signaling. *Blood*. 119:1810-1820.
Hume, D.A., P. Pavli, R.E. Donahue, and I.J. Fidler. 1988. The effect of human recombinant macrophage colony-stimulating factor (CSF-1) on the murine mononuclear phagocyte system in vivo. *J Immunol*. 141:3405-3409.
Huynh, J., M.Q. Kwa, A.D. Cook, J.A. Hamilton, and G.M. Scholz. 2012. CSF-1 receptor signalling from endosomes mediates the sustained activation of Erk1/2 and Akt in macrophages. *Cell Signal*. 24:1753-1761.
Irvine, K.M., C.J. Burns, A.F. Wilks, S. Su, D.A. Hume, and M.J. Sweet. 2006. A CSF-1 receptor kinase inhibitor targets effector functions and inhibits pro-inflammatory cytokine production from murine macrophage populations. *FASEB journal : official publication of the Federation of American Societies for Experimental Biology*. 20:1921-1923.
Jenkins, S.J., and J.E. Allen. 2010. Similarity and diversity in macrophage activation by nematodes, trematodes, and cestodes. *Journal of biomedicine & biotechnology*. 2010:262609.
Jenkins, S.J., D. Ruckerl, P.C. Cook, L.H. Jones, F.D. Finkelman, N. van Rooijen, A.S. MacDonald, and J.E. Allen. 2011. Local macrophage proliferation, rather than recruitment from the blood, is a signature of TH2 inflammation. *Science*. 332:1284-1288.
Kanitakis, J., P. Petruzzo, and J.M. Dubernard. 2004. Turnover of epidermal Langerhans' cells. *The New England journal of medicine*. 351:2661-2662.
Karp, C.L., and P.J. Murray. 2012. Non-canonical alternatives: what a macrophage is 4. *The Journal of experimental medicine*. 209:427-431.
Klein, I., J.C. Cornejo, N.K. Polakos, B. John, S.A. Wuensch, D.J. Topham, R.H. Pierce, and I.N. Crispe. 2007. Kupffer cell heterogeneity: functional properties of bone marrow derived and sessile hepatic macrophages. *Blood*. 110:4077-4085.
Landberg, G., E.M. Tan, and G. Roos. 1990. Flow cytometric multiparameter analysis of proliferating cell nuclear antigen/cyclin and Ki-67 antigen: a new view of the cell cycle. *Exp Cell Res*. 187:111-118.
Le Goff, L., T.J. Lamb, A.L. Graham, Y. Harcus, and J.E. Allen. 2002. IL-4 is required to prevent filarial nematode development in resistant but not susceptible strains of mice. *Int J Parasitol*. 32:1277-1284.
Lenda, D.M., E. Kikawada, E.R. Stanley, and V.R. Kelley. 2003. Reduced macrophage recruitment, proliferation, and activation in colony-stimulating factor-1-deficient mice results in decreased tubular apoptosis during renal inflammation. *J Immunol*. 170:3254-3262.
Liao, X., N. Sharma, F. Kapadia, G. Zhou, Y. Lu, H. Hong, K. Paruchuri, G.H. Mahabeleshwar, E. Dalmas, N. Venteclef, C.A. Flask, J. Kim, B.W. Doreian, K.Q. Lu, K.H. Kaestner, A. Hamik, K. Clement, and M.K. Jain. 2011. Kruppel-like factor 4 regulates macrophage polarization. *The Journal of clinical investigation*. 121:2736-2749.
Linde, N., W. Lederle, S. Depner, N. van Rooijen, C.M. Gutschalk, and M.M. Mueller. 2012. Vascular endothelial growth factor-induced skin carcinogenesis

depends on recruitment and alternative activation of macrophages. *J Pathol*. 227:17-28.
Loke, P., I. Gallagher, M.G. Nair, X. Zang, F. Brombacher, M. Mohrs, J.P. Allison, and J.E. Allen. 2007. Alternative activation is an innate response to injury that requires CD4+ T cells to be sustained during chronic infection. *J Immunol*. 179:3926-3936.
Lu, B., B.J. Rutledge, L. Gu, J. Fiorillo, N.W. Lukacs, S.L. Kunkel, R. North, C. Gerard, and B.J. Rollins. 1998. Abnormalities in monocyte recruitment and cytokine expression in monocyte chemoattractant protein 1-deficient mice. *The Journal of experimental medicine*. 187:601-608.
MacDonald, K.P., J.S. Palmer, S. Cronau, E. Seppanen, S. Olver, N.C. Raffelt, R. Kuns, A.R. Pettit, A. Clouston, B. Wainwright, D. Branstetter, J. Smith, R.J. Paxton, D.P. Cerretti, L. Bonham, G.R. Hill, and D.A. Hume. 2010. An antibody against the colony-stimulating factor 1 receptor depletes the resident subset of monocytes and tissue- and tumor-associated macrophages but does not inhibit inflammation. *Blood*. 116:3955-3963.
Martinez, F.O., S. Gordon, M. Locati, and A. Mantovani. 2006. Transcriptional profiling of the human monocyte-to-macrophage differentiation and polarization: new molecules and patterns of gene expression. *J Immunol*. 177:7303-7311.
Mohrs, K., D.P. Harris, F.E. Lund, and M. Mohrs. 2005. Systemic dissemination and persistence of Th2 and type 2 cells in response to infection with a strictly enteric nematode parasite. *J Immunol*. 175:5306-5313.
Murphy, J., R. Summer, A.A. Wilson, D.N. Kotton, and A. Fine. 2008. The prolonged life-span of alveolar macrophages. *Am J Respir Cell Mol Biol*. 38:380-385.
Murray, P.J., and T.A. Wynn. 2011. Protective and pathogenic functions of macrophage subsets. *Nature reviews. Immunology*. 11:723-737.
Nguyen, K.D., Y. Qiu, X. Cui, Y.P. Goh, J. Mwangi, T. David, L. Mukundan, F. Brombacher, R.M. Locksley, and A. Chawla. 2012. Alternatively activated macrophages produce catecholamines to sustain adaptive thermogenesis. *Nature*. 480:104-108.
Noben-Trauth, N., G. Kohler, K. Burki, and B. Ledermann. 1996. Efficient targeting of the IL-4 gene in a BALB/c embryonic stem cell line. *Transgenic research*. 5:487-491.
Pello, O.M., M. De Pizzol, M. Mirolo, L. Soucek, L. Zammataro, A. Amabile, A. Doni, M. Nebuloni, L.B. Swigart, G.I. Evan, A. Mantovani, and M. Locati. 2011. Role of c-MYC in alternative activation of human macrophages and tumor-associated macrophage biology. *Blood*. 119:411-421.
Priceman, S.J., J.L. Sung, Z. Shaposhnik, J.B. Burton, A.X. Torres-Collado, D.L. Moughon, M. Johnson, A.J. Lusis, D.A. Cohen, M.L. Iruela-Arispe, and L. Wu. 2010. Targeting distinct tumor-infiltrating myeloid cells by inhibiting CSF-1 receptor: combating tumor evasion of antiangiogenic therapy. *Blood*. 115:1461-1471.
Ruckerl, D., S.J. Jenkins, N.N. Laqtom, I.J. Gallagher, T.E. Sutherland, S. Duncan, A.H. Buck, and J.E. Allen. 2012. Induction of IL-4Ralpha-dependent microRNAs identifies PI3K/Akt signaling as essential for IL-4-driven murine macrophage proliferation in vivo. *Blood*.
Schulz, C., E. Gomez Perdiguero, L. Chorro, H. Szabo-Rogers, N. Cagnard, K. Kierdorf, M. Prinz, B. Wu, S.E. Jacobsen, J.W. Pollard, J. Frampton, K.J. Liu,

and F. Geissmann. 2012. A lineage of myeloid cells independent of Myb and hematopoietic stem cells. *Science*. 336:86-90.
Smith, J.L., A.E. Schaffner, J.K. Hofmeister, M. Hartman, G. Wei, D. Forsthoefel, D.A. Hume, and M.C. Ostrowski. 2000. ets-2 is a target for an akt (Protein kinase B)/jun N-terminal kinase signaling pathway in macrophages of motheaten-viable mutant mice. *Molecular and cellular biology*. 20:8026-8034.
Tagliani, E., C. Shi, P. Nancy, C.S. Tay, E.G. Pamer, and A. Erlebacher. 2011. Coordinate regulation of tissue macrophage and dendritic cell population dynamics by CSF-1. *The Journal of experimental medicine*. 208:1901-1916.
Thomas, G.D., D. Ruckerl, B.H. Maskrey, P.D. Whitfield, M.L. Blaxter, and J.E. Allen. 2012. The biology of nematode- and IL4Ralpha-dependent murine macrophage polarization in vivo as defined by RNA-Seq and targeted lipidomics. *Blood*.
Tushinski, R.J., I.T. Oliver, L.J. Guilbert, P.W. Tynan, J.R. Warner, and E.R. Stanley. 1982. Survival of mononuclear phagocytes depends on a lineage-specific growth factor that the differentiated cells selectively destroy. *Cell*. 28:71-81.
Ulich, T.R., J. del Castillo, L.R. Watson, S.M. Yin, and M.B. Garnick. 1990. In vivo hematologic effects of recombinant human macrophage colony-stimulating factor. *Blood*. 75:846-850.
Vats, D., L. Mukundan, J.I. Odegaard, L. Zhang, K.L. Smith, C.R. Morel, R.A. Wagner, D.R. Greaves, P.J. Murray, and A. Chawla. 2006. Oxidative metabolism and PGC-1beta attenuate macrophage-mediated inflammation. *Cell metabolism*. 4:13-24.
Verreck, F.A., T. de Boer, D.M. Langenberg, M.A. Hoeve, M. Kramer, E. Vaisberg, R. Kastelein, A. Kolk, R. de Waal-Malefyt, and T.H. Ottenhoff. 2004. Human IL-23-producing type 1 macrophages promote but IL-10-producing type 2 macrophages subvert immunity to (myco)bacteria. *Proceedings of the National Academy of Sciences of the United States of America*. 101:4560-4565.
Volkman, A., N.C. Chang, P.H. Strausbauch, and P.S. Morahan. 1983. Differential effects of chronic monocyte depletion on macrophage populations. *Lab Invest*. 49:291-298.
Wermeling, F., R.M. Anthony, F. Brombacher, and J.V. Ravetch. 2013. Acute inflammation primes myeloid effector cells for anti-inflammatory STAT6 signaling. *Proceedings of the National Academy of Sciences of the United States of America*. 110:13487-13491.
Wu, D., A.B. Molofsky, H.E. Liang, R.R. Ricardo-Gonzalez, H.A. Jouihan, J.K. Bando, A. Chawla, and R.M. Locksley. 2011. Eosinophils sustain adipose alternatively activated macrophages associated with glucose homeostasis. *Science*. 332:243-247.
Wurster, A.L., V.L. Rodgers, M.F. White, T.L. Rothstein, and M.J. Grusby. 2002. Interleukin-4-mediated protection of primary B cells from apoptosis through Stat6-dependent up-regulation of Bcl-xL. *The Journal of biological chemistry*. 277:27169-27175.
Yona, S., K.W. Kim, Y. Wolf, A. Mildner, D. Varol, M. Breker, D. Strauss-Ayali, S. Viukov, M. Guilliams, A. Misharin, D.A. Hume, H. Perlman, B. Malissen, E. Zelzer, and S. Jung. 2013. Fate mapping reveals origins and dynamics of

monocytes and tissue macrophages under homeostasis. *Immunity*. 38:79-91.

Figure 1. IL-4 drives CSF-1-independent MΦ proliferation.
(A) BL/6 mice were injected i.p. with IL-4c or PBS plus anti-CSF1R mAb (CSF1R), Rat IgG (RIgG) or PBS on d0 or d2. The proportion of F4/80^{High} pleural MΦ positive for Ki67, Ki67^{High} or RELMα and total MΦ numbers were determined by flow-cytometry on d2 after the last injection. Graphs depict individual data for 4 mice/group . **(B)** As (A) but on d3 after daily oral gavage with vehicle control or GW2580 on d0 to 3. **(C)** Mice were injected with single dose of PBS or IL-4c and the expression of CSF1R mRNA determined 24h later in FACS-purified F4/80^{High} peritoneal MΦ. *$P < 0.001$ determined by two-tailed *t* test. Individual data for 5 mice/group is shown. **(D)** CSF-1 levels in pleural lavage fluid and serum from mice in (A) determined by ELISA. All data are representative of 2-3 separate experiments, with the same results observed in the peritoneal cavity.

Figure 2. MΦ-intrinsic IL-4Rα signaling is essential for proliferation and alternative activation triggered by IL-4c. (A) *LysM^{cre}Il4ra$^{-/lox}$* BALB/c mice were injected i.p. on d0 and 2 with PBS or IL-4c and peritoneal lavage cells analyzed on d4 by flow cytometry for BrdU incorporation, or Ki67, RELMα and Ym1 versus F4/80 expression. Representative flow-cytograms gated on F4/80^{High} peritoneal MΦ with frequencies depicting the mean ± SEM of 4 mice per group. **(B)** *Il4ra$^{-/lox}$* (Het), *LysM^{cre}Il4ra$^{-/lox}$* (Lys) or *Il4ra$^{-/-}$* (-/-) BALB/c were treated with PBS (open) or IL-4c (filled) as in (A) and BrdU incorporation by F4/80^{High} pleural MΦ determined on d3 together with the frequency of BrdU^{+} cells in RELMα positive (+) or negative (-) F4/80^{High} MΦ from the IL-4c-treated *LysM^{cre}Il4ra$^{-/lox}$* group. *$P < 0.05$, **$P < 0.01$, and ***$P < 0.001$ determined by ANOVA (left graph) or paired *t* test (right graph). Data are representative of 4 independent experiments inclusive of data in (A), with 3-4 mice/group. **(C)** BL/6 *Il4ra$^{+/+}$Cd45.1^{+}Cd45.2^{+}* mice were lethally irradiated and reconstituted with a 50:50 mix of *Il4ra$^{+/+}$Cd45.1^{+}Cd45.2^{+}* and *Il4ra$^{-/-}$ Cd45.1^{null}Cd45.2$^{+/+}$* congenic BM cells. The frequency of blood monocytes (gated as side-scatter [SSC]^{Low} CD11b^{+} CD115^{+}) derived from each BM was determined by analysis of CD45.1 and CD45.2 expression 8 wk later. A representative flow cytogram of CD45.1 and CD45.2 expression on blood monocytes is shown together with a graph depicting the frequency of CD45.1^{+} and CD45.1^{-} monocytes in all blood leukocytes from 10 individual mice. **(D)** Mice from (C) were subsequently injected

i.p. twice, two days apart, with PBS or IL-4c and pleural lavage cells analyzed 2d after the last injection for CD45.1 and CD45.2 expression. Representative flow-cytograms gated on all live F4/80^{High} MΦ are shown together with a graph depicting the total number of *Il4ra*$^{+/+}$ *Cd45.1*$^{+}$ (closed circles) and *Il4ra*$^{-/-}$ *Cd45.1*^{null} (open circles) pleural F4/80^{High} MΦ in each group, with individual data for 5 mice/group presented. **(E)** Representative flow cytograms depicting CD45.1 expression versus BrdU incorporation or Ym1 expression gated on single F4/80^{High} CD19^{-} pleural MΦ from mice in (D), and graphs showing the proportion of *Il4ra*$^{+/+}$ *Cd45.1*$^{+}$ (closed circles) and *Il4ra*$^{-/-}$ *Cd45.1*^{null} (open circles) F4/80^{High} CD19^{-} MΦ positive for BrdU or Ym1 for individual mice. (C-E) Representative of 2 experiments.

Figure 3. IL-4Rα-dependent and independent mechanisms of proliferation during nematode infection. (A) BL/6 mice were given a single i.p. injection of IL-13c, IL-4c or PBS and the proportion of BrdU^{+}, Ki67^{+}, and RELMα^{+} F4/80^{High} peritoneal MΦ determined 36hr later. Graphs depict individual data for 6 mice per group and are representative of 2 independent experiments. Horizontal bars indicate median values. Equivalent results were obtained in the pleural cavity. **P* < 0.05, ***P* < 0.01, and ****P* < 0.001 determined by Kruskal-Wallis test. **(B)** C57BL/6 (WT) and *Il4ra*$^{-/-}$ (-/-) mice were infected with *Ls* and the total number of F4/80^{High} pleural MΦ and the proportion positive for BrdU, Ki67, and RELMα determined on d10. Results pooled from 2 experiments with 15-16 mice/group shown. ***P* < 0.01 and ****P* < 0.001 determined by ANOVA. **(C)** BL/6 mice were given a single i.p. dose of IL-4c (solid line) or PBS (dashed line), following which the total number of pleural cavity F4/80^{High} MΦ and the proportion positive for RELMα, Ki67^{High} or Ki67, were determined over a 4d time course. Data are mean ± SEM of 4 mice/group, representative of 2 experiments, and with the same results obtained for peritoneal MΦ. Day zero represents naïve. **(D)** As (C) but from *Ls*-infected (solid line) or naïve (dashed line) mice. Data are mean ± SEM from 4-5 mice per group and representative of 3 experiments. **(E)** Representative flow cytograms of F4/80^{High} peritoneal MΦ 4d after a single i.p. injection of PBS or IL-4c containing 5, 1.25, or 0.31 μg of IL-4 on d0 and 2. Frequencies are means with SEM in brackets of 3-6 IL-4c-treated animals per group, or a single value for pooled cells from 3 PBS-treated mice. A repeat using a single injection regime verified dose effect for both of IL-4c and IL-13c.

Figure 4. Elevated CSF-1 production contributes to MΦ proliferation during tissue nematode infection. (A) BL/6 mice were infected with *Ls* and injected i.p. on d8 with anti-CSF1R mAb (CSF1R), Rat IgG (RIgG) or PBS. Total number of F4/80^{High} pleural MΦ and the proportion positive for BrdU, Ki67 or Ym1 were determined on d10. Data is pooled from 2 experiments with 7, 13, and 20 mice for naïve, PBS and RIgG treated infected, and anti-CSFR1-treated infected, groups respectively. *$P < 0.05$ and **$P < 0.01$ determined by Kruskal-Wallis test. **(B)** CSF-1 levels in pleural lavage (left) or serum (right) from mice in (A) determined by ELISA. (A&B) Horizontal bars indicate median.

Figure 5. IL-4Rα signaling to MΦ provides a competitive advantage during tissue nematode infection. (A) BL/6 *Il4ra*$^{+/+}$*Cd45.1*$^{+}$*Cd45.2*$^{+}$ mice were lethally irradiated and reconstituted with a 50:50 mix of *Il4ra*$^{+/+}$*Cd45.1*$^{+}$*Cd45.2*$^{+}$ and *Il4ra*$^{-/-}$ *Cd45.1*^{null}*Cd45.2*$^{+/+}$ congenic BM cells over 8 wk. Mice were infected with *Ls* following which BrdU incorporation or Ym1 expression versus expression of CD45.1 was determined on single F4/80^{High} CD19^{-} pleural MΦ at d10 and 16 post-infection. Representative flow cytograms are shown, while graphs depict the proportion of IL-4Rα^{+} CD45.1^{+} (closed squares) and IL-4Rα^{-} CD45.1^{-} (open squares) cells positive for BrdU or Ym1, with each line illustrating paired measurements from individual mice. Data pooled from 2 experiments, with 11-12 mice/group. ***$P < 0.001$ determined by paired *t* test. **(B)** CD45.1 and CD45.2 expression gated on all F4/80^{High} pleural MΦ from mice in (A) and graphical presentation of the total number of IL-4Rα^{+} CD45.1^{+} (closed squares) and IL-4Rα^{-} CD45.2$^{+/+}$ (open squares) subsets of these cells. *$P <$ 0.05, **$P < 0.01$, and ***$P < 0.001$ determined by Kruskal-Wallis test. Horizontal bars indicate median values. **(C)** Frequency of IL-4Rα^{+} CD45.1^{+} cells within CD115^{+} CD11b^{+} SSC^{Low} blood monocytes and pleural cavity eosinophils (SSC^{High}, F4/80^{Low}, MHCII^{-}), DC (CD11c^{High} MHCII^{High}) and F4/80^{High} MΦ at d10 and 16 post-infection of mice in (A), with lines joining cells of individual mice. **(D)** *Il4ra*$^{+/+}$ (WT), *Il4ra*$^{-/lox}$ (Het), *LysM*^{cre}*Il4ra*$^{-/lox}$ (Lys) or *Il4ra*$^{-/-}$ (-/-) mice were infected with *Ls* or left naïve and RELMα and IL-4Rα staining on F4/80^{High} pleural MΦ determined at d17. Frequencies are means with SEM in brackets of 5-7 mice/group. The emergence of RELMα^{+} MΦ in *LysM*^{cre}*Il4ra*$^{-/lox}$ mice was confirmed in a further 3 independent

experiments between d14 and 60 post-infection. **(E)** C57BL/6 (WT) or *Rag1*$^{-/-}$ (-/-) mice were infected with *Ls* and the total number of pleural cavity F4/80^{High} MΦ and the proportion incorporating BrdU or expressing Ym1 was determined on d10, with mean and SEM of 5 mice/group shown. **(F)** As (E) but both peritoneal (PeC) and pleural (PleC) cavity F4/80^{High} MΦ from naïve (open circles) or *Ls*-infected C57BL/6 mice were analyzed at 10d post-infection. Representative of 3 experiments with 8 mice/group. *$P < 0.05$ and **$P < 0.01$ determined by Kruskal-Wallis test. Horizontal bars indicate median values.

Figure 6. IL-4 dependent proliferation occurs during GI nematode infection and provides a competitive advantage to IL-4Rα^{+} MΦ.

(A) BALB/c mice were infected orally with *Hp* and peritoneal lavage cells assessed at d7. Representative flow cytograms of all peritoneal cells showing gates and frequencies for all, or BrdU^{+}, Ki67^{+}, RELMα^{+} or Ym1^{+}, F4/80^{High} MΦ. Representative of 5 experiments. **(B)** BALB/c (WT) or *Il4*$^{-/-}$ (-/-) mice were infected with *Hp* (closed symbols) or left naïve (open symbols) and the total peritoneal F4/80^{High} MΦ and the proportion positive for BrdU, Ki67, Ym1, and RELMα^{+}, determined on d7. Representative of 3 experiments with 3-4 mice per group. *$P <$ 0.05, **$P < 0.01$ and ***$P < 0.001$ determined by ANOVA. **(C)** As (B) but following treatment of BALB/c mice with anti-CSF1R mAb (CSF1R) or Rat IgG (IgG) on d6. **(D)** *Il4ra*$^{+/+}$*Cd45.1*$^{+}$*Cd45.2*$^{+}$ mice were lethally irradiated and reconstituted for 8 wk with a 50:50 mix of *Il4ra*$^{+/+}$*Cd45.1*$^{+}$*Cd45.2*$^{+}$ and *Il4ra*$^{-/-}$ *Cd45.1*^{null}*Cd45.2*$^{+}$ congenic BM cells before infection with *Hp*. The frequency of CD45.1^{+} cells in different leukocyte subsets in the peritoneal cavity in naïve (open symbols) and *Hp*-infected mice (closed symbols) was determined on d7 and 14 post-infection. The graph shows total numbers of *Il4ra*$^{+/+}$ *Cd45.1*$^{+}$ and *Il4ra*$^{-/-}$ *Cd45.1*^{null} peritoneal F4/80^{High} MΦ obtained in naïve (open) and infected (closed) mice at each time-point. **(E)** *Il4ra*$^{-/lox}$ (Het), *LysM*^{cre}*Il4ra*$^{-/lox}$ (Lys) or *Il4ra*$^{-/-}$ (-/-) mice were infected with *Hp* and RELMα expression by F4/80^{High} peritoneal MΦ determined on d14 and 28. (C-E) Data are from independent experiments performed once and are confirmatory of data from the *Ls* model.

Figure 7. CSF-1 but not IL-4 stimulates neutrophil and monocyte recruitment alongside elevated proliferation of resident tissue MΦ. (A) BL/6 mice were injected i.p. with PBS (open circles), Fc-CSF-1 (closed squares) or IL-4c (closed triangles) and Ki67 and RELMα expression by F4/80^{High} peritoneal MΦ determined 24h later. Representative flow cytograms show all live peritoneal lavage cells. Data representative of 2 independent experiments. **(B)** Total Ly-6C^{+} CD115^{+} monocytes and Ly-6C^{Intermediate} SSC^{Intermediate} neutrophils in peritoneal lavage cells from mice in (A), and representative flow-cytograms depicting gating strategies. Upper flow-cytograms also depict CD115^{+} Ly6C^{-} monocytes/MΦ (left-hand gate) and lower flow-cytograms show SSC^{High} Ly6C^{Low} eosinophil gate, both of which exhibited no change in total number.

Figure S1. Ex vivo S phase MΦ are distinguished by high levels of Ki67 expression. (A) BL/6 mice were injected with PBS or IL-4c on d0 and 2 and peritoneal cavity F4/80^{High} MΦ analyzed on d4 for Ki67 expression versus BrdU incorporation. Frequency of cells expressing high levels of Ki67 (italics) is approximate to those positive for BrdU (Roman text). Gates distinguishing positive events were set using isotype control staining (Ki67) or the absence of DNase treatment (BrdU). Representative of pleural and peritoneal MΦ from 4 separate experiments. **(B)** BL/6 mice were given a single i.p. injection of IL-4c or PBS and single F4/80^{High} CD19^{-} MΦ from peritoneal and pleural cavities were assessed over the following 96h period for proliferation and alternative activation. Representative flow cytograms depict the gates used to determine the frequency of Ki67^{+}, Ki67^{High}, RELMα^{+} and Ym1^{+} cells, with the proportion of F4/80^{High} MΦ in cell cycle or S phase determined as Ki67^{+} or Ki67^{High}, respectively. Of note, control injection of PBS led to a small but significant increase in proliferation of MΦ in the peritoneal cavity injection site but not in the pleural cavity suggesting that 27G needle stick injury drives MΦ into cycle, with ramifications for methodologies used to directly manipulate tissue sites and study MΦ functions. Data is from the same experiment as that shown in Fig. 3C.

Figure S2. Dissociation of cell aggregates for analysis of F4/80^{High} MΦ composition. (A) FSC-A vs FSC-W plots of pleural cavity cells from PBS or IL-4c

treated animals showed that between 20-25% of events are doublets. The majority of these were B cell:B cell events (data not shown) but the second most common were B cell:MΦ doublets, identified as F4/80^{High} CD19^{+}. The proportion of MΦ in doublets with B cells increased greatly to almost 50% upon treatment with IL-4c, and appeared mainly formed of cells expressing the highest levels F4/80, suggesting a wild-type CD45.1^{+} phenotype. (B) Less than 10% of pleural cavity events were doublets when Accumax cell aggregate dissociation medium was used prior to fixation. Almost all remaining doublets were B cell:B cell interactions (data not shown), with B-cell:MΦ doublets reduced to ≤ 10% of all F4/80^{High} events. However, to further prevent bias induced by these remaining doublets, the CD45.1^{+} CD45.2^{+} cell gate was set to exclude events that deviated from the expected linear relationship between CD45.1 and CD45.2 on this population. The absence of such events on dot-plots from which doublets had been excluded using a FSC-A vs FSC-W gate confirmed them to be doublets of CD45.1^{-} CD45.1^{+} and CD45.1^{+} CD45.2^{+} cells. Analysis of MΦ CD45.1/CD45.2 composition was performed on all live F4/80^{High} cells (R1), whereas analysis of proliferation and alternative activation was performed on CD19^{-} F4/80^{High} cells gated on single events (R2).

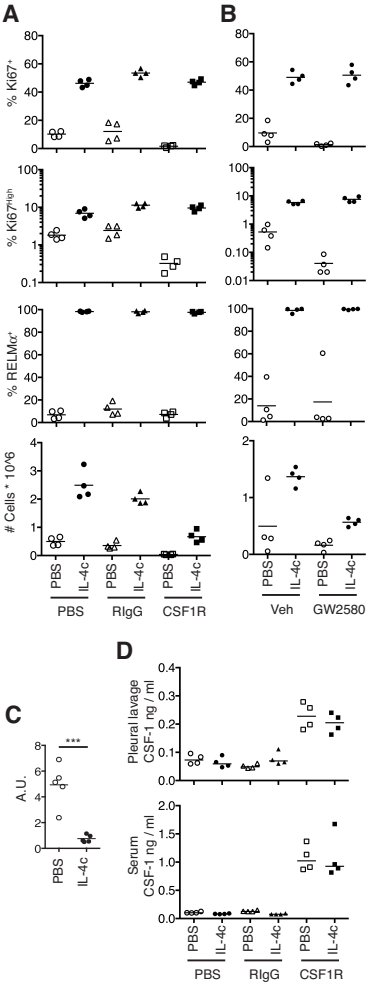
A
B
% Ki67+
% Ki67high
% RELMα+
# Cells * 10^6
PBS
IL-4c
PBS
RIgG
CSF1R
Veh
GW2580
C
A.U.
***
D
Pleural lavage CSF-1 ng / ml
Serum CSF-1 ng / ml

Figure 1

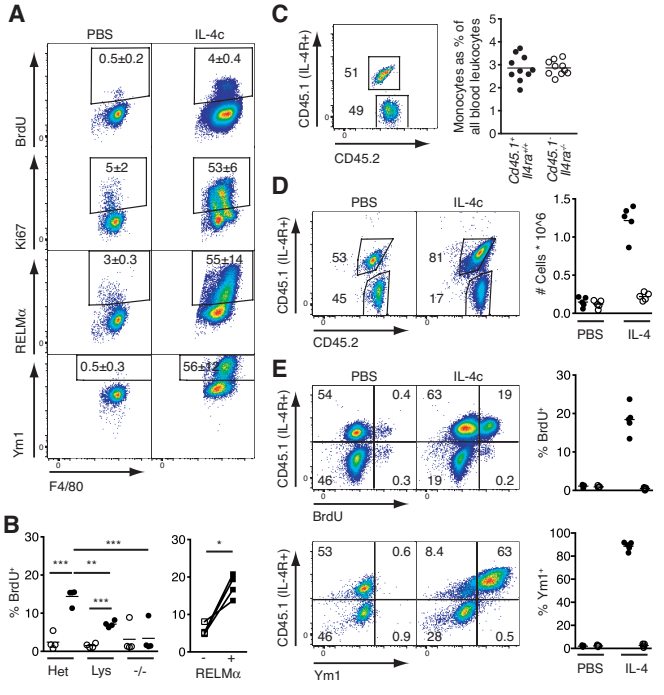
A
PBS
IL-4c
BrdU
Ki67
RELMα
Ym1
F4/80
0.5±0.2
4±0.4
5±2
53±6
3±0.3
55±14
0.5±0.3
56±12
B
% BrdU+
Het
Lys
-/-
RELMα
C
CD45.1 (IL-4R+)
CD45.2
51
49
Monocytes as % of all blood leukocytes
Cd45.1+ Il4ra+/+
Cd45.1- Il4ra-/-
D
53
45
81
17
Cells * 10^6
PBS
IL-4
E
54
0.4
63
19
46
0.3
19
0.2
BrdU
% BrdU+
53
0.6
8.4
63
46
0.9
28
0.5
Ym1
% Ym1+

Figure 2

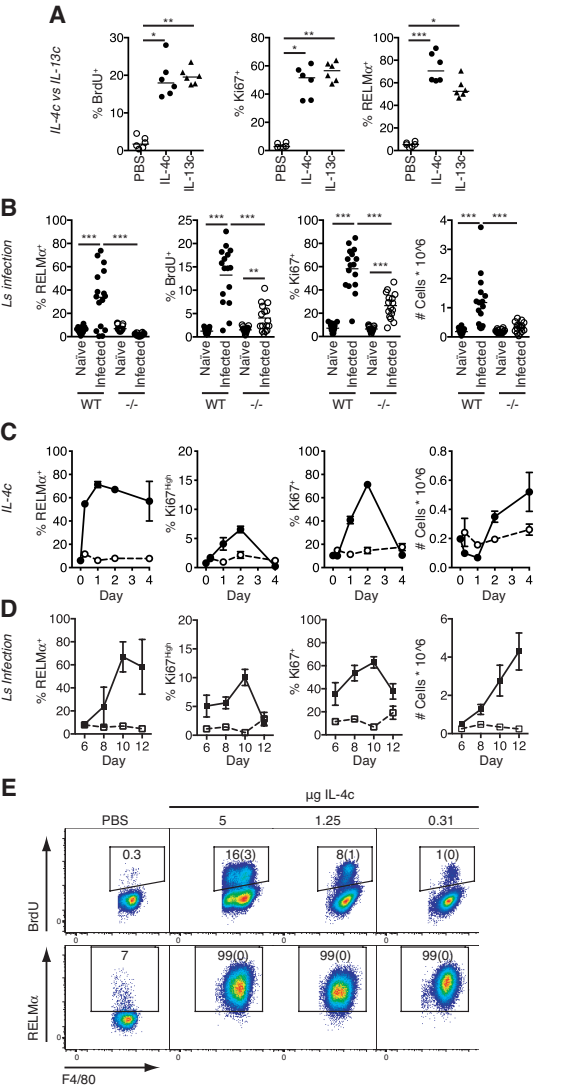
A
IL-4c vs IL-13c
% BrdU+
% Ki67+
% RELMα+
PBS
IL-4c
IL-13c
B
Ls infection
% RELMα+
% BrdU+
% Ki67+
# Cells * 10^6
Naive
Infected
WT
-/-
C
IL-4c
% RELMα+
% Ki67high
% Ki67+
# Cells * 10^6
Day
D
Ls Infection
% RELMα+
% Ki67hi
% Ki67+
# Cells * 10^6
Day
E
μg IL-4c
PBS
5
1.25
0.31
BrdU
RELMα
F4/80
0.3
16(3)
8(1)
1(0)
7
99(0)
99(0)
99(0)

Figure 3

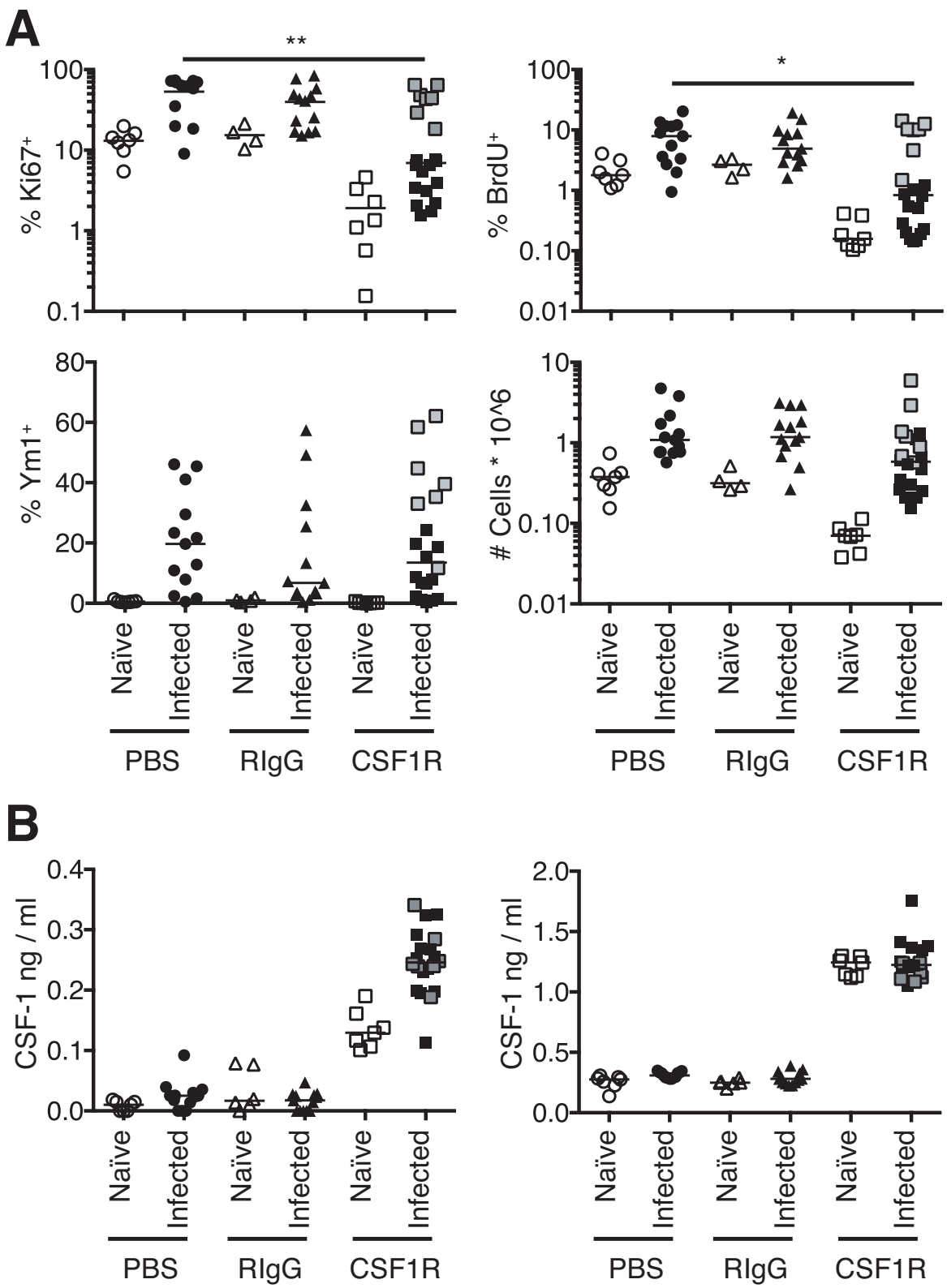
A
**
*
% Ki67+
% BrdU+
% Ym1+
# Cells * 10^6
100
10
1
0.1
0.01
80
60
40
20
0
Naïve
Infected
PBS
RIgG
CSF1R
B
CSF-1 ng / ml
0.4
0.3
0.2
0.1
0.0
2.0
1.5
1.0
0.5

Figure 4

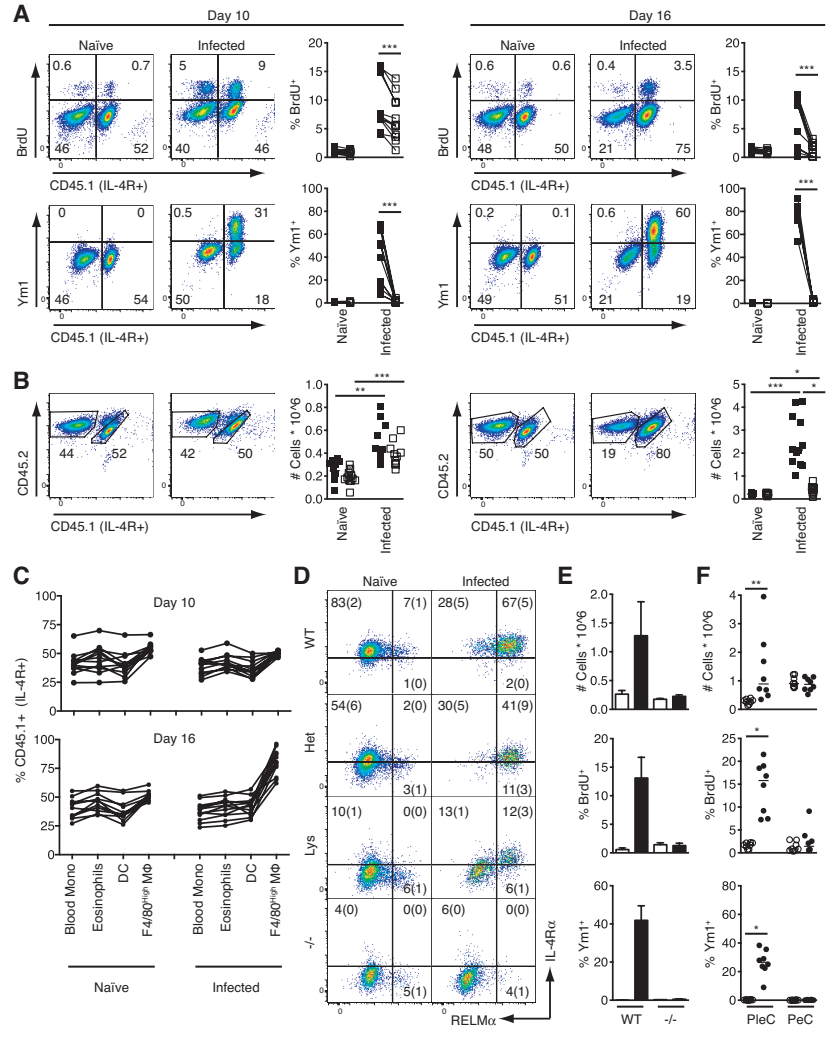
A
Day 10
Day 16
Naïve
Infected
BrdU
CD45.1 (IL-4R+)
% BrdU+
Ym1
% Ym1+
B
CD45.2
Cells * 10^6
C
% CD45.1+ (IL-4R+)
Blood Mono
Eosinophils
DC
F4/80high Mφ
D
WT
Het
Lys
-/-
IL-4Rα
RELMα
E
WT
-/-
F
PleC
PeC

Figure 5

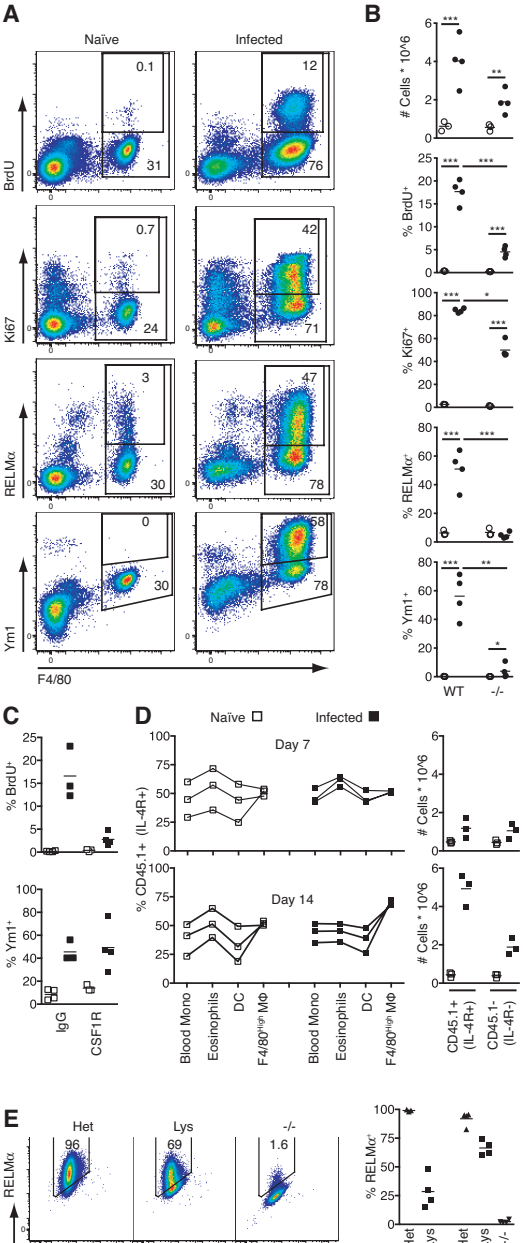
A
Naïve
Infected
BrdU
Ki67
RELMα
Ym1
F4/80
0.1
31
12
76
0.7
24
42
71
3
30
47
78
0
30
58
78
B
Cells * 10^6
% BrdU+
% Ki67+
% RELMα+
% Ym1+
WT
-/-
C
% BrdU+
% Ym1+
IgG
CSF1R
D
Naïve
Infected
Day 7
Day 14
% CD45.1+ (IL-4R+)
# Cells * 10^6
Blood Mono
Eosinophils
DC
F4/80high Mϕ
CD45.1+ (IL-4R+)
CD45.1- (IL-4R+)
E
Het
Lys
-/-
96
69
1.6
RELMα
Autofluorescence
% RELMα+
Day 14
Day 28

Figure 6

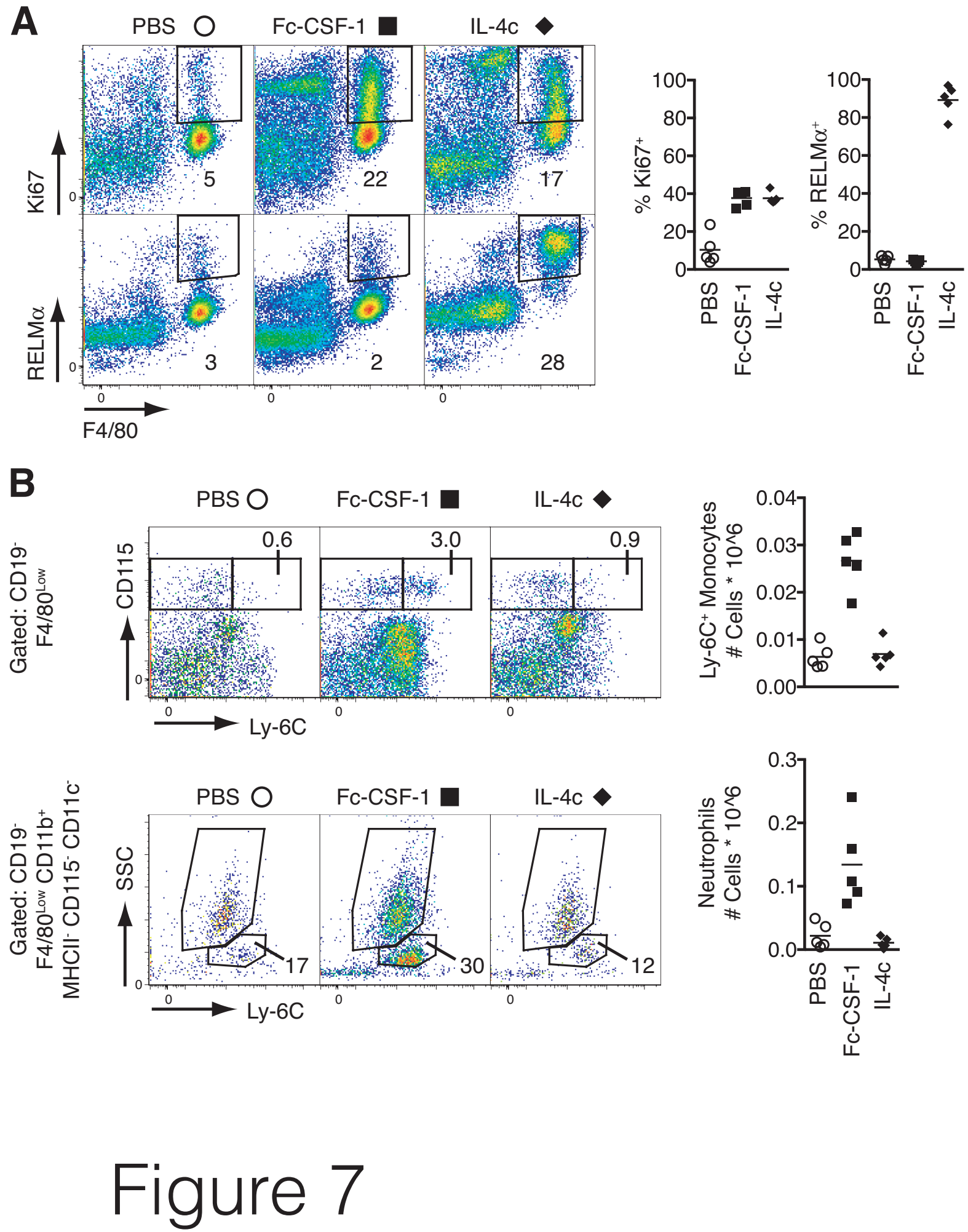
A
PBS
Fc-CSF-1
IL-4c
Ki67
RELMα
F4/80
5
22
17
3
2
28
% Ki67+
% RELMα+
100
80
60
40
20
0
PBS
Fc-CSF-1
IL-4c
B
Gated: CD19- F4/80Low
CD115
Ly-6C
0.6
3.0
0.9
Ly-6C+ Monocytes
Cells * 10^6
0.04
0.03
0.02
0.01
0.00
Gated: CD19- F4/80Low CD11b+ MHCII- CD115- CD11c-
SSC
17
30
12
Neutrophils
Cells * 10^6
0.3
0.2
0.1
0.0

Figure 7

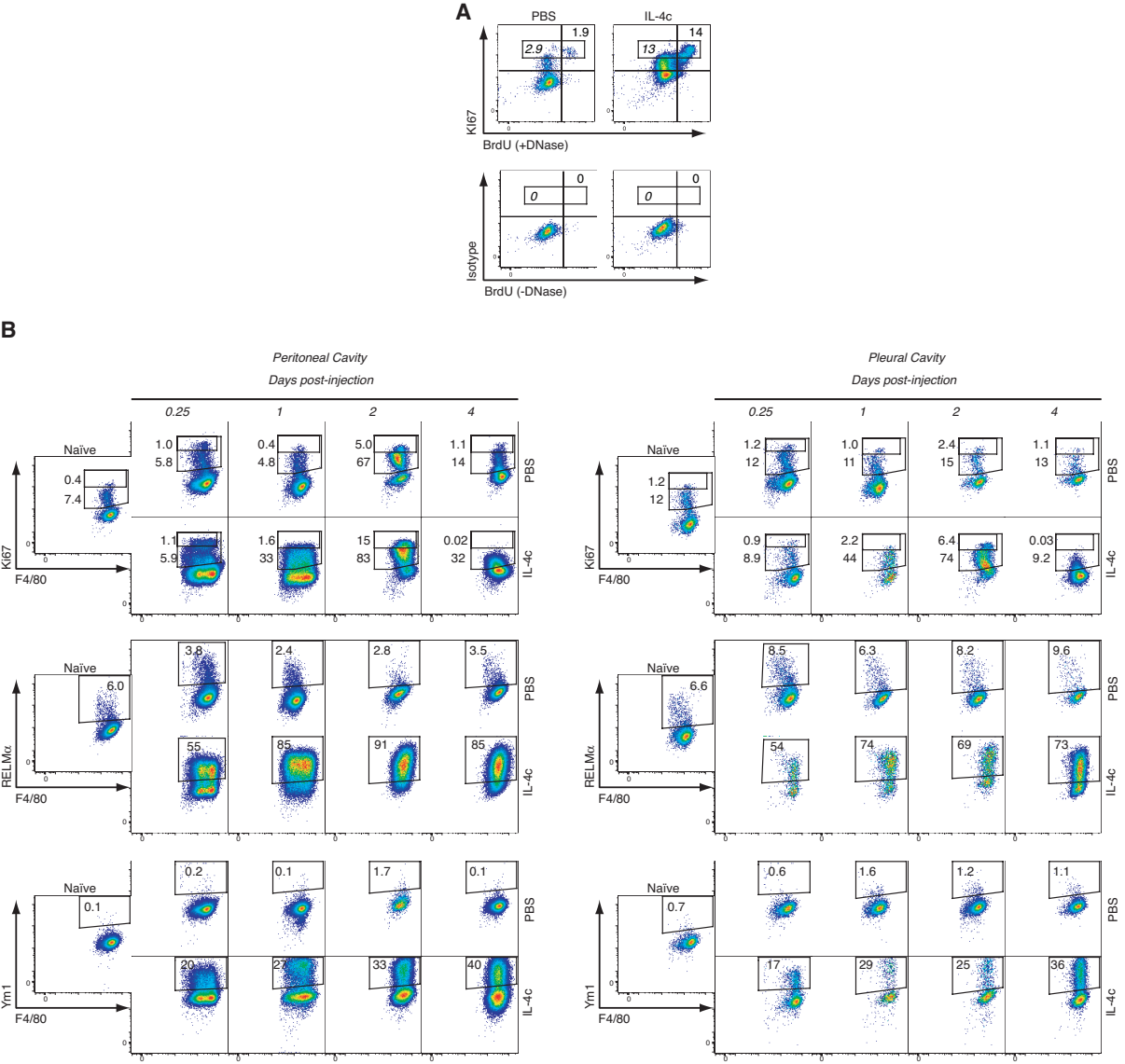
A
PBS
IL-4c
1.9
2.9
14
13
Ki67
BrdU (+DNase)
0
0
Isotype
BrdU (-DNase)
B
Peritoneal Cavity
Days post-injection
Pleural Cavity
0.25
1
2
4
Naïve
PBS
IL-4c
F4/80
Ki67
RELMα
Ym1

Figure S1

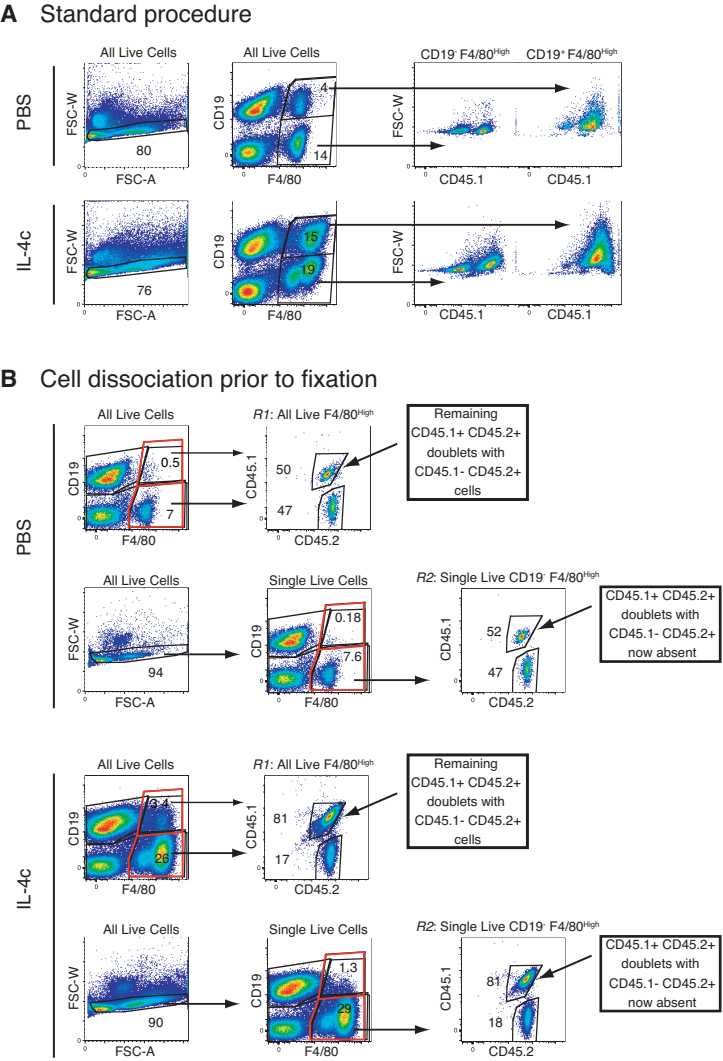
A
Standard procedure
PBS
IL-4c
All Live Cells
FSC-W
FSC-A
80
76
CD19
F4/80
4
14
15
19
CD19⁻ F4/80High
CD19⁺ F4/80High
CD45.1
B
Cell dissociation prior to fixation
R1: All Live F4/80High
CD45.2
0.5
7
50
47
Remaining CD45.1+ CD45.2+ doublets with CD45.1- CD45.2+ cells
Single Live Cells
94
0.18
7.6
R2: Single Live CD19⁻ F4/80High
52
CD45.1+ CD45.2+ doublets with CD45.1- CD45.2+ now absent
6.4
26
81
17
90
1.3
23
18

Figure S2